npj | Flexible Electronics

www.nature.com/npjflexelectron

REVIEW ARTICLE OPEN

Check for updates

Recent developments of advanced micro-supercapacitors: design, fabrication and applications

Fan Bu[1,3], Weiwei Zhou[2,3], Yihan Xu[2], Yu Du[2], Cao Guan[1]✉ and Wei Huang[1]✉

The rapid development of wearable, highly integrated, and flexible electronics has stimulated great demand for on-chip and miniaturized energy storage devices. By virtue of their high power density and long cycle life, micro-supercapacitors (MSCs), especially those with interdigital structures, have attracted considerable attention. In recent years, tremendous theoretical and experimental explorations have been carried out on the structures and electrode materials of MSCs, aiming to obtain better mechanical and electrochemical properties. The high-performance MSCs can be used in many fields, such as energy storage and medical assistant examination. Here, this review focuses on the recent progress of advanced MSCs in fabrication strategies, structural design, electrode materials design and function, and integrated applications, where typical examples are highlighted and analyzed. Furthermore, the current challenges and future development directions of advanced MSCs are also discussed.

npj Flexible Electronics (2020)4:31 ; https://doi.org/10.1038/s41528-020-00093-6

INTRODUCTION

With the rapid development of modern science and technology, the application of electronic products is also expanding at an extremely high speed. In order to improve people's living standards, some intelligent, flexible and miniaturized electronic products and components are gradually emerging in the industry, such as folding mobile phones, health trackers and micro sensors, intelligent robots and other micro systems. With the integration of these miniaturized microelectronic devices and intelligent autonomous systems in various applications, developing small energy storage devices matched well to them is becoming highly urgent[1–5].

At present, portable devices mainly rely on micro-batteries and micro-supercapacitors (MSCs) as power sources. Typically, they can be integrated with miniaturized electronic devices and provide them with the required power and energy for a period of time. In particular, MSCs have generated more and more interest in certain fields require long lifetime and fast charge/discharge rate. For instance, in biomedical and sensor fields, micro-batteries inevitably suffer from frequent replacement due to their short life-span (only a few hundred to several thousand times). Apart from the economic and environmental problems caused, in some cases like powering implantable biochips, this may even need a surgery to accomplish such a replacement process. In contrast, MSCs can work for an ultralong time (usually thousands of times continuously) with only a small capacitance attenuation, which can effectively avoid the frequent replacement problem[6–8]. Additionally, micro-batteries are not competent in the cases high power is needed. Although it has been reported that high power can be output to integrated systems through series and/or parallel connection of batteries, it will inevitably increase the device volume. Clearly, this is against the original intention of designing micro system. Unlike micro-batteries, MSCs can demonstrate much higher power density in a small volume without additional integration measures, which is quite suitable for flexible integrated systems requiring high power density[9–12]. Moreover, the adoption of highly flexible substrates makes planar MSCs capable of gaining excellent mechanical properties. Thus, it is found that MSCs are more skilled and have higher practicability than micro-batteries in these particular areas[13–16]. Currently, MSCs have two types of structures: conventional sandwich structures and in-plane interdigital structures (Fig. 1)[17]. Normally, the interdigitated coplanar electrode architecture tends to exhibit better rate capability and higher power density than the sandwich structure. This is supposed to be ascribed to its special structure that greatly shortens the ion diffusion distance of electrolyte and provides a higher active surface area[18–20]. Inspired by this, it is necessary to summarize and discuss the influence of device structure on the performance of MSCs.

Nowadays, owing to more and more investigations on MSCs, progresses on high-performance devices emerge one after another. Nevertheless, the low energy density is still a severe obstacle limiting their practical application. In fact, there are two key factors for the development of high-performance MSCs. Designing the electrode materials of the devices can be a pivotal factor. As a large number of studies have shown, reasonable design of the materials is potential to improve the electrochemical performance of the device[21–23]. The choice of electrode materials is of great importance toward enhancing the performances of MSCs, and the intrinsic properties of these materials are especially crucial to concern. Different types of materials have disparate characteristics, but good conductivity, high activity surface area as well as beneficial ion diffusion channels should be commonly acquired, in order to achieve great electrochemical properties. On the other hand, we can improve the performance of MSCs by optimizing the structures of all parts of the device (i.e. electrode, electrolyte, substrate and collector). The realization of this goal involves the selection and improvement of device manufacturing methods. At present, many miniaturized machining technologies can be used to fabricate planar MSCs. And the designs and manufactures of finger electrodes and electrolytes of MSCs are closely related to whether they can be used as a kind of excellent micro energy storage device in electronic components[17,24,25]. Therefore, in this review, we mainly introduce structural design,

[1]Institute of Flexible Electronics, Northwestern Polytechnical University, Xi'an 710072, China. [2]School of Materials Science and Engineering, Harbin Institute of Technology at Weihai, Weihai 264209, China. [3]These authors contributed equally: Fan Bu, Weiwei Zhou. ✉email: iamcguan@nwpu.edu.cn; iamwhuang@nwpu.edu.cn

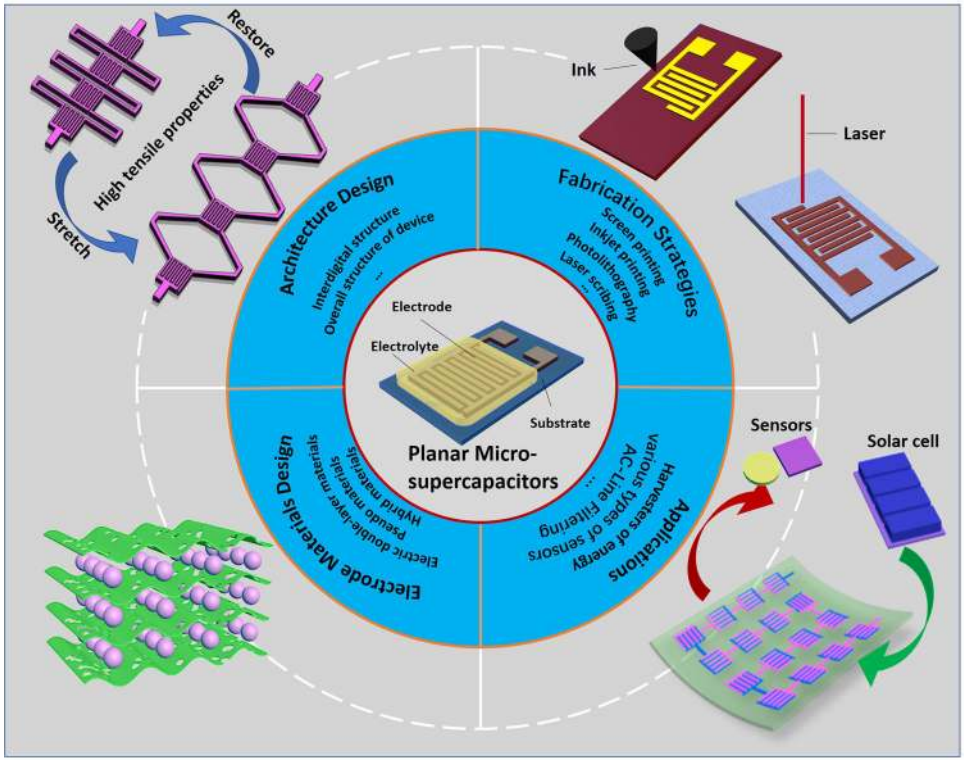

Fig. 1 Schematic illustrations of the components of MSCs and summary of this paper. Figures represent the composition of MSCs and main content of this article.

fabrication methods and applications of advanced MSCs, and also summarize various electrode materials and their optimal design in detail. On the whole, this review starts with describing the design concepts of MSCs' topology, and then introduces the reported fabrication methods to produce MSCs based on. Afterward, different types of active materials, including carbon-based materials, conducting polymer materials, metal-based materials and their optimal design are reviewed. Finally, we summarize the applications of MSCs and prospect its future development.

DEVICE ARCHITECTURE DESIGN

At present, there are two kinds of MSCs: traditional sandwich-structure MSCs and interdigital-structure MSCs. For a conventional sandwich MSC, it is a vertical structure composed of two electrodes and electrolyte sandwiched in the middle. Its performance mainly depends on the thickness of the separator and electrode layer. In order to obtain better electrochemical performance, the most effective way is to increase the load of active materials. However, due to the limitation of its structure, this requirement can only be achieved by increasing electrode thickness. In this way, the pathway of ion diffusion will be definitely lengthened, thereby resulting in lower power density[26].

Whereas, for MSCs with in-plane interdigital electrode architecture, electrodes are separated by insulated gap (Fig. 1), which gives rise to a few advantages. First of all, separators are no longer used, which means ions can achieve higher diffusion efficiency. Secondly, due to the special finger electrode structure, the transport of electrolyte ions mainly occurs in transverse direction. Therefore, the capacitance and energy density of MSCs can be increased by increasing electrode thickness without affecting the power density. Thirdly, the integration on the plane is beneficial to application of system and practical production of industry[26,27]. In all, the interdigital structure can meet the needs of social development and life more perfectly. Therefore, a great amount of attention has been paid to the research of interdigital-structure MSCs.

The performance of an interdigital-structure MSC mainly depends on the electrode width, thickness and gap size, which has been illustrated in a few works[28]. For example, Li et al.[29] found that when other conditions were the same, the current density based on the overall device area increased as the finger width rose from 300 to 600 μm. But when only the electrode area was considered, the areal capacitance decreased when the fingers were wider than 500 μm. This may be ascribed to the fact that, instead of improved conductivity, increased diffusion length becomes the dominant factor when the finger width is too high. On the other hand, with the increase of thickness, the areal capacitance continuously mounted. Therefore, by designing a reasonable device structure, the highest areal capacitance reaching ~ 0.7 mF cm^{-2} could be obtained. Similarly, Chih et al.[30] achieved an all-solid-state MSC with excellent performance by optimizing the structure and size of the device. Specifically, with the optimized electrode width, gap width, etc., an all solid-state MSC exhibited high areal (7.7 mF cm^{-2}) and volumetric (77.3 mF cm^{-3}) capacitances.

The above findings can be explained as follows. For the insulated gap, larger electrode interspacing will reduce ion diffusion efficiency and lead to the decrease of power density. For the electrode, too small width will cause lacking of active area of electrode materials, while excessive width will cause long diffusion length. All of these may result in the drop of capacitance. Therefore, in order to achieve better performance, we need to narrow the electrode interspacing and choose an appropriate electrode width. Generally speaking, increasing the ratio of electrode width to gap width (W_e/W_g) can effectively diminish equivalent series resistance (ESR) and also enhance power density and energy density[26].

In addition, in order to obtain higher flexibility that meets the demands of development of wearable devices and intelligent systems, MSCs with better tensile properties have been manufactured. Inspired by Kirigami patterning, Jiao et al.[31] successfully manufactured all-solid-state MSC arrays (MSCAs) with excellent mechanical properties. The fabrication only relied on the made of MXene/bacterial cellulose (BC) composite papers, followed by a simple laser-cutting process. The prepared MSCAs exhibited an areal capacitance of 111.5 mF cm^{-2} and good tensile, bending and twisting properties. The excellent tensile properties enabled MSCAs to adapt to a variety of complex application scenarios.

In a word, inspired by the above elaborately-designed MSCs with excellent performances, together with the change rules between the performances and structural parameters, we believe the design of the structures of MSCs is helpful to improve their electrochemical performances and broaden their practical applications. And these designs can be the adjustment and optimization of intrinsic parameters (like electrode width, thickness, gap width, etc.) of MSCs, and also the overall configuration of MSCs (like Kirigami superstructure, etc.).

BRIEF INTRODUCTION OF DEVICE REACTION MECHANISM

MSCs can be classified in several ways, such as the mechanism of energy storage, the choice of electrolyte and the type of electrode materials. Depending on the energy storage mechanisms, MSCs can be divided into two categories.

(1) Electric double-layer capacitors (EDLCs), in which the capacitance is produced by the double-layer structure formed by ions at the interface between electrolyte and electrode. During charging, the surfaces of two electrode surfaces will be positively or negatively charged under the action of external electric field, and then they will attract the oppositely charged ions from the electrolyte. When the electric field is scattered, the mutual attraction between the charges helps to form a stable electric double-layer, and the energy is stored in this process. During the discharging process, electrons flow from the negative to the positive electrode through the load, generating a current in the external circuit and the energy is correspondingly released[32–34]. Porous carbon materials are characteristic electrodes of EDLCs owing to their high specific surface areas that can contributing considerable EDL capacitance.

(2) Pseudo-supercapacitors, which rely on rapid adsorption/desorption or redox reactions to generate capacitance. During charging, the ions will gather on the interface of electrodes/solution under the applied electric field, and then a reversible redox reaction takes place in the electrode. At the same time, the energy is stored. And during discharging, the ions will be released from the electrode surface, and the stored energy will also be released through the external circuit. In general, as ions can enter into the electrodes and participate in the redox reactions, the capacitance of pseudo-supercapacitors is 10–100 times higher than double-layer capacitance, which only utilize the surface to storage charges[32,35]. Pseudo-supercapacitors normally employ metal compounds and conducting polymer as electrode materials, which can offer rich faradic reactions.

DEVICE PREPARATION METHODS

When the finger electrodes and devices are fabricated by different methods, the obtained electrochemical performances can vary significantly. This suggests that the preparation technology itself may have great influence on the device properties, probably due to the following reasons. Firstly, for a specific kind of electrode material, just a small change of fabrication method would result in various microstructures, which affects the device properties from the point of the transport ability of ions and electrons. Secondly, it is well known that the electrochemical performance of MSCs depends on both the width of electrodes and the interspace between a pair of electrodes. And the accuracy of the above parameters will be also swayed by fabrication methods, causing the distinction of electrochemical performance. Therefore, in this section, some of the typical fabrication methods ever reported for patterning electrode finger arrays are reviewed. And the advantages and disadvantages of each strategy will be compared and analyzed to provide guidance for manufacturing high-performance MSCs.

Screen printing

Screen printing is a technology that uses ink to print the specific patterns on the substrates with the help of screen. It has the merits of rapidness, simplicity and low cost, and there are various types of substrates that can be directly printed on. Therefore, this method is quite suitable for MSCs manufacturing, especially in mass production[36–38]. The common strategy of screen printing involves printing active electrode materials and current collector separately. For example, as shown in Fig. 2a, Chih et al.[30] reported an all-screen-printable method to fabricate all-solid-state flexible MSCs. After screen-printing the hybrid electrodes of graphene/CNTs, an additional Ag current collector was then screen-printed on the top of the electrode layer. Finally, using a 2 M electrolyte of H_3PO_4/PVA, the resultant MSC (finger and interspace width of 0.5 mm and 0.8 mm, respectively) achieved a high areal capacitance of 7.7 mF cm^{-2} and volumetric capacitance of 77.3 F cm^{-3} at 5 mV s^{-1}, and excellent cyclic stability of >99% capacity retention after 15,000 cycles, which could be credited to the effective combination of graphene and CNT (Fig. 2b). Recently, Liu et al.[39] successfully constructed a flexible symmetrical MSC via first screen-printing Au current collector followed by Ag@polypyrrole (Ag@Ppy) ink, as shown in Fig. 2c. After dropping the gel electrolyte, the fabricated MSC exhibited excellent electrochemical performance in terms of high energy density (4.33×10^{-3} mWh cm^{-2}) and favorable cycle stability, as well as good mechanical flexibility.

In addition, screen printing can also print MXene materials. For example, Yu et al.[40] developed crumpled nitrogen-doped MXene (MXene-N) nanosheets via a melamine formaldehyde templating method. By throughout the optimization of the ink viscosity, they fabricated MSCs based on MXene-N nanosheets through screen printing. Due to the nitrogen doping and crumpled structures enhanced conductivity and redox activity, the MSCs delivered an areal capacitance of 70.1 mF cm^{-2} and outstanding mechanical robustness. In another case, by making the segments of unelected cursor and multilayered MXene into aqueous inks, Abdolhosseinzadeh et al.[41] successfully fabricated a MSC on paper, as shown in Fig. 2d. And this method enabled the resulting MSCs to show much superior areal capacitance (158 mF cm^{-2}). For screen printing, large-batch production in an extremely short time is one of its greatest merits that is hard to accomplish for other fabrication methods. Moreover, the step-by-step printing of both electrode materials and electrolytes enabled by screen printing may provide a way to fabricate all-solid-state MSCs. But at the same time, it should also be noticed that the preparation of electrode materials ink and its low resolution are still the challenges that need to be addressed, in order to further promote the application potential of screen printing.

Inkjet printing

Inkjet printing is a technology involves spraying ink on the surface of substrates to obtain various patterns. Compared with other technologies, it owns the advantages of high precision, feasibility of room temperature manufacturing as well as the capacity of mass production. Moreover, it can also print the electrode material directly on the substrate, making it especially suitable for the fabrication of functional thin films in applications of solar cells,

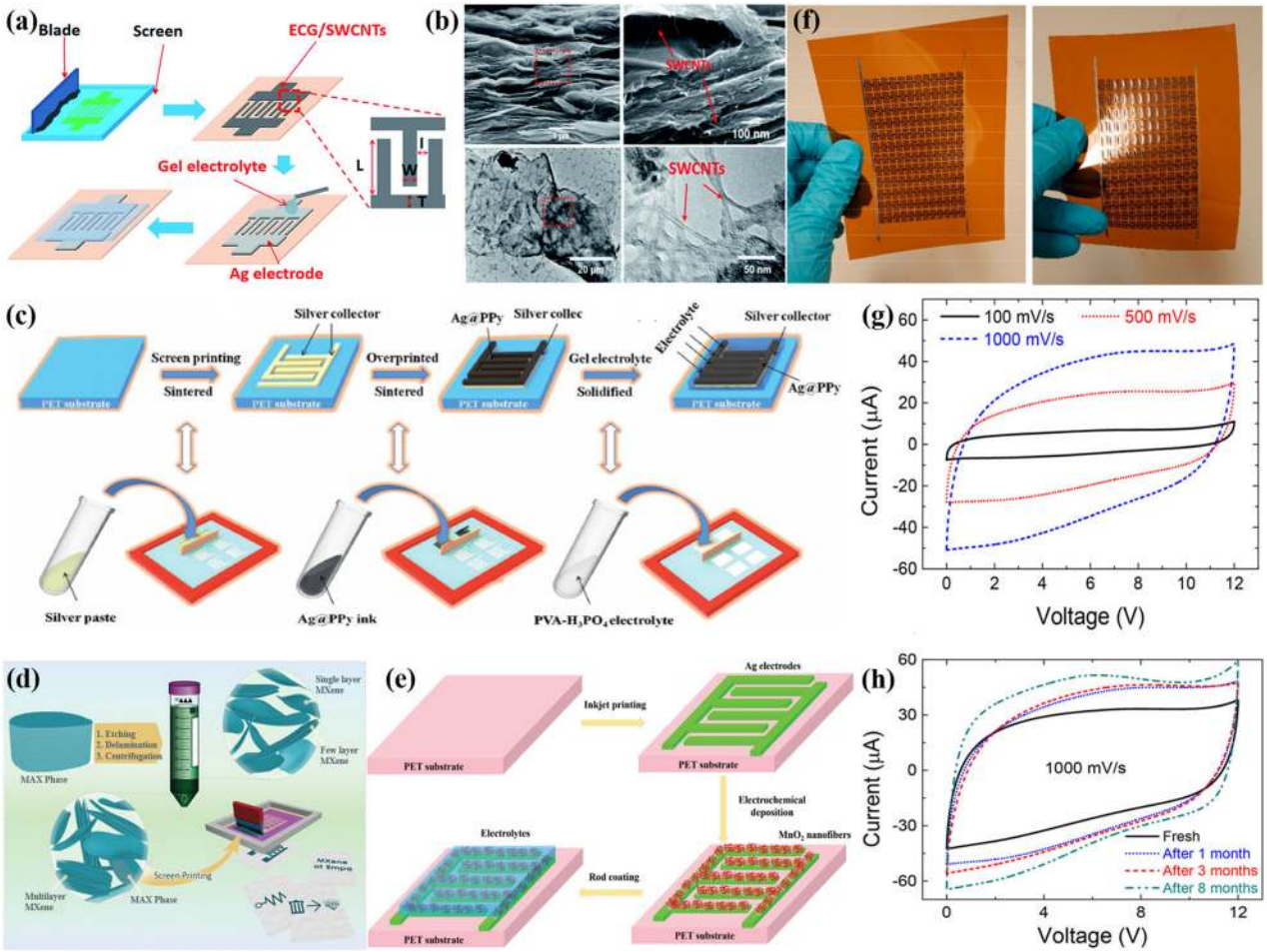

Fig. 2 Fabrication methods of screen printing and inkjet printing. a Schematic illustration for preparing the all screen-printable MSCs. **b** SEM images for the graphene/CNTs hybrid electrodes. **c** Fabrication process of the Ag@Ppy ink-based MSCs. **d** Schematic illustration of direct screen printing of MXene sediments. **e** Fabrication of the flexible MSCs with MnO_2 porous nanofiber-like electrodes. **f** Photos of large-scale integration of fully printed MSCs on Kapton. CV profiles of the MSC array at **g** different scan rates and **h** different periods. **a**, **b** Reproduced with permission[30] (Copyright © 2019, Royal Society of Chemistry). **c** Reproduced with permission[39] (Copyright © 2017, John Wiley and Sons). **d** Reproduced with permission[41] (Copyright © 2020, John Wiley and Sons). **e** Reproduced with permission[52] (Copyright © 2019, John Wiley and Sons). **f**–**h** Reproduced with permission[29] (Copyright © 2017, American Chemical Society).

electrochemical energy storage devices and so on[42–49]. In the fabrication process, the key of inkjet printing is to prepare the ink with appropriate fluidity. The most common way is to configure the ink of electrode material, and then directly print it on the substrate to obtain MSCs. For example, Wang et al.[50] prepared a high performance and flexible MSC by printing the ink with three-dimensional (3D) metal-ion-doped MnO_2 nanosheets. Thanks to the introduction of metal ions, electrochemical performance of the prepared device was greatly enhanced. In addition, Pang et al.[51] fabricated asymmetric MSCs with graphene nanosheets and lamellar $K_2Co_3(P_2O_7)_2 \cdot 2H_2O$ nanomaterials as cathodes and anodes respectively by inkjet printing. And the prepared MSC exhibited a high volume capacitance of 6.0 F cm^{-3}.

In addition to the traditional inkjet printing technique involving direct use of active material ink, the combination of inkjet printing and other methods, such as electrochemical deposition, is also a feasible method. For example, Cheng et al.[52] first prepared interdigital Ag electrodes on PET substrates by inkjet printing. Then, porous nanofiber-like electrode structures were obtained by electrochemically depositing MnO_2 on the Ag electrodes as shown in Fig. 2e. Benefiting from the electrode structures, the prepared MSC delivered a high areal capacitance of 46.6 mF cm^{-2} and 86.8% capacitance reserved after 1000 times of bending to 180°.

Note that inkjet printing can also be used to fabricate large-scale MSC arrays quickly and easily. For example, Li et al.[29] successfully integrated a multiple MSC by inkjet printing method, which solved the problem of low voltage usually occurred in a single device and thus making it more practical. Specifically, they fabricated MSCs based on graphene by a simple full-inkjet-printing technique. By optimizing the electrode thickness and other parameters, the prepared MSCs could attain a high areal capacitance of 0.7 mF cm^{-2}. More importantly, more than 100 devices (Fig. 2f) could be successfully connected as power banks in this approach, which enabled effective integration of large-scale MSC arrays. And the MSC arrays could be charged up to 12 V (Fig. 2g) and retained the performance even for the long span of 8 months (Fig. 2h), confirming their excellent electrochemical and integration properties.

To sum up, although the production efficiency of inkjet printing is inferior to that of screen printing, the high resolution can be its most significant advantage. In addition, inkjet printing also allows a wide selection range of substrates and electrode materials, which may bring opportunities for fabricating high-performance flexible MSCs. Moreover, high voltage window and energy density can be obtained by printing large scale integrated MSCs on flexible substrates. This is quite important for the practical

application of MSCs in high voltage systems. Through the precise control of electrodes size and gaps together with the improvement of ink quality, inkjet printing can be further developed and is hopeful to promote the fabrication of high performance MSCs.

Photolithography

Photolithography is a method of making patterns with photoresist, which can not only achieve high resolution of the products, but also produce various complex plane patterns. Thus, it is often used to provide templates for electrode materials of MSCs[53–56]. For example, as shown in Fig. 3a, Sun et al.[57] first prepared the single-wall carbon nanotube (SWNT) /carbon current collectors via carbonization process that converted the photoresist into amorphous carbon on SWNT. After further growth of MnO_2 nanostructures, in-plane MSC with a high stack capacitance of 20.4 F cm^{-3} was prepared. Moreover, the combination of photolithography with pyrolysis-reduction can also bring about high-performance MSCs, as reported by Hong et al.[58] They created porous carbon/tin quantum dots (C/Sn QDs), which could serve both as the electrode active materials and as the current collector. Importantly, the Sn QDs with high electrical conductivity allowed the fabricated MSC to deliver a higher areal specific capacitance of 5.79 mF cm^{-2} than that of C-MSC. And it could retain 93.3% capacitance even after 5,000 cycles, indicating its desirable cycling stability.

Another instance of involving more than just photolithography to prepare high-performance MSCs can be the work of Tian et al.[59], as illustrated in Fig. 3b. They first fabricated the interdigital patterns and Ti/Au layer on SiO_2 substrate by photolithography and physical vapor deposition (PVD) techniques, and then deposited the holey graphene oxide intermediate layer on the current collectors via a drop dry technique, followed by electropolymerizing the uppermost polyaniline layer. The ingenious combination of these preparation methods enabled the as-prepared MSCs to show a high stack capacitance of 271.1 F cm^{-3}, high energy density of 24.1 mWh cm^{-3} and good rate capability.

All in all, photolithography is regarded as a good candidate to manufacture various types of precision MSCs with good electrochemical performance. Owing to its high resolution and mature operation process, photolithography is widely used in small integrated systems to ensure their high accuracy. However, due to the limitations of technology itself, it is necessary to be combined with other technologies to accomplish the whole manufacturing process. In addition, the template (photoresist) has to be removed in buffer solution or at high temperature. These will result in low efficiency and difficulty for large-scale production, which greatly limits its development. What's worse, high cost and the pollution of photoresist reagents are also problems hindering its practical application, so the development of photolithography method still has a way to go.

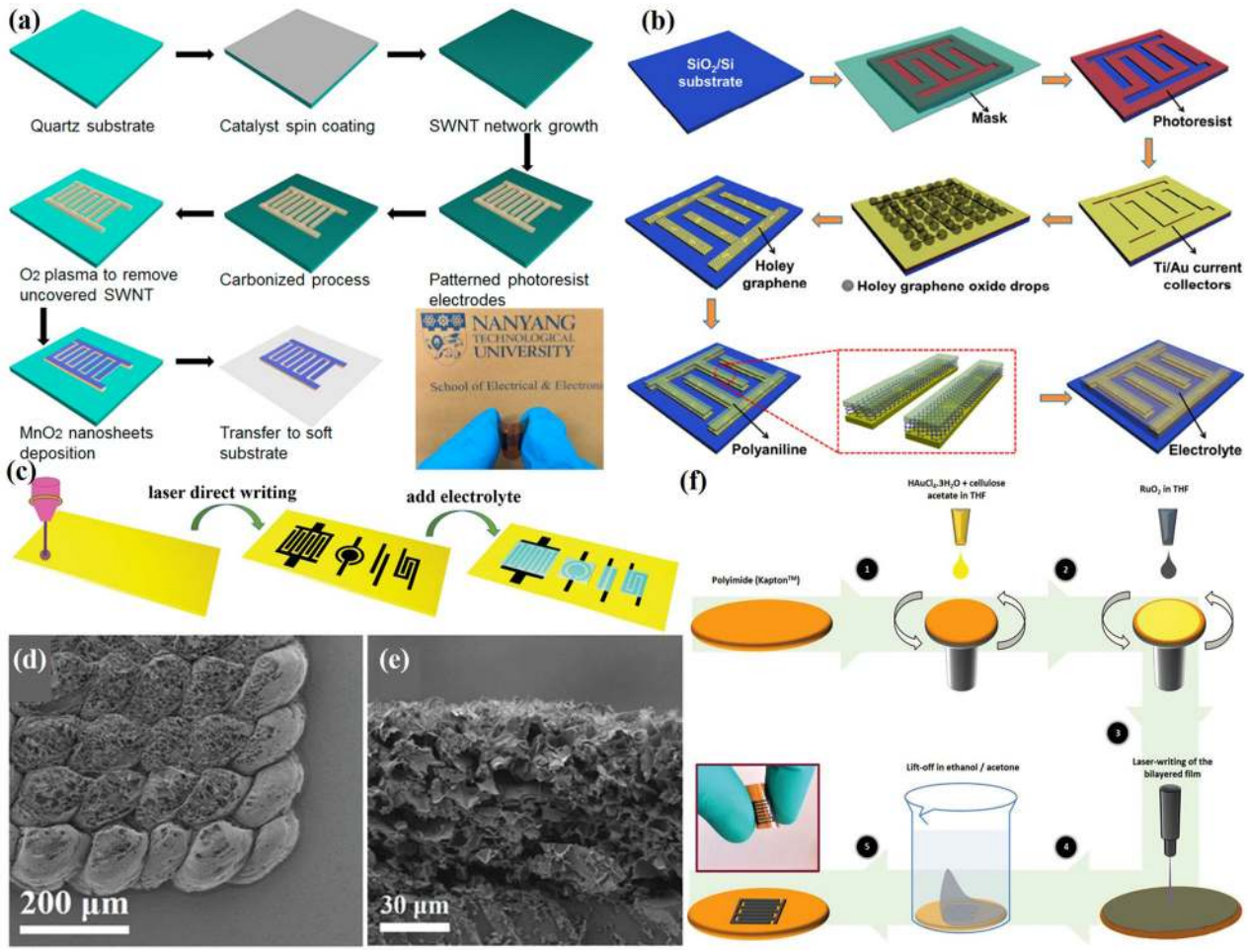

Fig. 3 Photolithography and laser scribing for fabricating MSCs. Schematic illustration of fabrication process for **a** SWNT/carbon/MnO_2-based MSC on a soft substrate; **b** MSCs with holey graphene/polyaniline heterostructures. **c** Fabrication of LIG films for MSCs by laser scribing. **d** Top-view and **e** cross-section SEM images of LIG films. **f** Fabrication process of RuO_2-based flexible MSCs. **a** Reproduced with permission[57] (Copyright © 2016, Elsevier). **b** Reproduced with permission[59] (Copyright © 2016, Springer Nature). **c**–**e** Reproduced with permission[66] (Copyright © 2019, John Wiley and Sons). **f** Reproduced with permission[68] (Copyright © 2019, John Wiley and Sons).

Laser scribing

Laser scribing is to use high-energy laser beam to irradiate on the surface of the workpiece to make the irradiated area locally melted and gasified, so as to achieve the purpose of scribing. Owning to its simplicity, high precision and high speed, laser scribing has been commonly applied in the manufacture of MSCs[60–64]. For example, Peng et al.[65] reported the successful preparation of boron-doped porous graphene simply by laser induction, which was transformed from the polyimide sheets immersed in boric acid. After assembling with a solid-state electrolyte, the flexible solid-state MSC could be readily fabricated, and the resulting devices exhibited a high areal capacitance of 16.5 mF cm^{-2}, 3 times higher than the devices with non-doped electrode materials. Similarly, Shi et al.[66] demonstrated a one-step, cost-effective, and scalable production of laser-induced graphene (LIG) micropatterns through laser scribing (production process shown in Fig. 3c). Significantly, the laser scribing process toward the commercial polyimide (PI) membrane could simultaneously achieve the fabrication and the patterning of LIG films (Fig. 3d, e), which was quite suitable for highly integrated MSCs free of metal current collectors, interconnects, or extra substrate. When a polymer gel of PVA/H_3PO_4 was used as the electrolyte, the resulting LIG-MSCs showed a great areal capacitance of 0.62 mF cm^{-2} and good cycle stability with no loss of capacitance after 10,000 cycles. Moreover, this method also avoided the complexity and high cost of traditional manufacturing process, and was more conducive to practical applications of MSCs. In addition, Li et al.[67] prepared flexible MSCs with excellent electrochemical performance by combining laser induction with electrodeposition technology. Such an integration provides a reference for the preparation of high performance MSCs.

Figure 3f shows another example, in which Brousse et al.[68] fabricated flexible MSCs based on ruthenium oxide (RuO_2) on PI foil using a simple approach by laser-writing of a bilayered film. Due to the pillar morphology of electrodes, the fabricated MSC delivered high capacitances of 27 mF cm^{-2}/540 F cm^{-3} in 1 M H_2SO_4, and it also presented high cycle performance, retaining 80% capacitance after 10,000 cycles. In another instance, Jiang et al.[69] carried out a simple laser scribing treatment to large-area benzene-bridged Ppy film synthesized by interfacial polymerization. The obtained MSCs using 1-ethyl-3-methylimidazolium tetrafluoroborate as the electrolyte could achieve a high energy of up to 50.7 mWh cm^{-3} and power density of 9.6 kW cm^{-3}.

In brief, unlike photolithography, laser scribing omits the use of additional templates and complex processes. In addition, laser scribing can not only accomplish the direct transformation of commercial polymer films into graphene and other active materials, but also induce the formation of active materials, such as metal oxides. Thus, it has occupied a place in the preparation of micro energy storage devices and especially been deemed as an effective manufacture method to fabricate high-capacitance MSCs. Moreover, laser scribing can also achieve good tensile properties of the obtained MSCs, according to the work of Jiao et al.[31]. Therefore, laser scribing has been widely used in the manufacture of various types of MSCs devices, and has been placed large expectations for the manufacture of those with high performances.

Mask-assisted filtering

Mask-assisted filtering is a method to obtain MSCs or microbatteries by vacuum filtration of the liquid electrode active material with the assistance of template. The method is concise, easy-operated, and low-cost compared to other methods[70,71]. Recently, Huang et al.[72] reported a simple and effective method to exfoliate multilayer-MXene via the gentle water freezing-and-thawing (FAT) approach, and massive FAT-MXene flakes (reaching 39%) could be obtained after four cycles of this procedure. Then the FAT-MXene could be used to fabricate on-chip all-MXene MSC by template-assisted filtering (Fig. 4a). Due to the large amount of FAT-MXene of this synthesis strategy, the obtained MSC exhibited high areal capacitance of 23.6 mF cm^{-2} and volumetric capacitance of 591 F cm^{-3} with the optimal electrode thickness, as shown in Fig. 4b.

It is also very simple and convenient to make asymmetrical MSCs (AMSCs) through mask-assisted filtering. For example, as shown in Fig. 4c, Qin et al.[73] first deposited graphene current collectors on the mask, then added the solution containing mesoporous MnO_2 nanosheets (prepared by a bottom-up self-assembly strategy) and the solution of porous VN nanosheets onto different sides of the mask. After a simple mask-assisted deposition method followed coating the gel electrolyte, all-solid-state AMSC was obtained, with mesoporous MnO_2 nanosheets and porous VN nanosheets as the positive and the negative electrodes, respectively. It is noteworthy that the as-prepared AMSC showed an impressive energy density of 21.6 mWh cm^{-3}, long-term cycling stability and a broad voltage window of 2 V (Fig. 4d). Besides, Zheng et al.[74] took a maskassisted filtration strategy to make the urchin-like sodium titanate and the nanoporous activated graphene deposited on either side of the MSC, respectively. After applying high-voltage ion gel as the electrolyte, the planar sodium-ion micro-capacitors (NIMCs) were obtained on a flexible substrate, which exhibited a high volumetric energy density, excellent mechanical flexibility as well as good heat resistance at 80 °C. What's more, the NIMCs could also self-discharge for 44 h from V_{max} to 0.6 V_{max}, proving the good electrochemical performance.

As it can be seen, mask-assisted filtering is undoubtedly a good way to fabricate MSCs because of its convenience and efficiency to deposit not only active materials but also current collectors. Also, it does not require extra ink preparation or expensive equipment, thereby providing a simple pathway toward high performance MSCs. However, the preparation of masks is bound to be a time-consuming task, thereby limiting its development and application more or less. In addition, the substrate of MSCs obtained by mask-assisted filtration is confined to filter membrane. Additional transfer processes are normally required to transfer MSCs to other substrates (like PET, PI, etc.), which directly limits the selection range of substrates and consumes the preparation time.

Other fabrication methods

In addition to the methods listed above, there are some additional promising ways that can be used to make MSCs. For example, through a scalable, low-cost stamping strategy, Zhang et al.[75] produced flexible MSCs based on 2D MXene. In a typical fabrication process, they first used 3D printing technology to make the templates in the required shapes, followed by imprinting MXene ink on the substrate as shown in Fig. 4e and f. After coating electrolyte, the flexible all-MXene MSC were produced, which could deliver a high areal capacitance of 61 mF cm^{-2} at 25 μA cm^{-2} and showed excellent mechanical capability (Fig. 4g). Importantly, the stamping strategy reported by this work provides an idea for mass production of flexible MSCs. In addition, Zhu et al.[76] used medical adhesive tapes as the substrates through a simple pencil drawing method combined with deposition of MnO_2 solution, the electrode materials were readily prepared. After coating the solid-state electrolyte, the solid-state MSC showed excellent mechanical and electrochemical properties as well as good biocompatibility.

Moreover, the combination of coating and automated scalpel technology is also a promising preparation method for planar MSCs. For example, Salles et al.[77] first prepared MXene thin films via dip coating. Then, through an automated scalpel technique, coplanar MSCs with different levels of transparency were

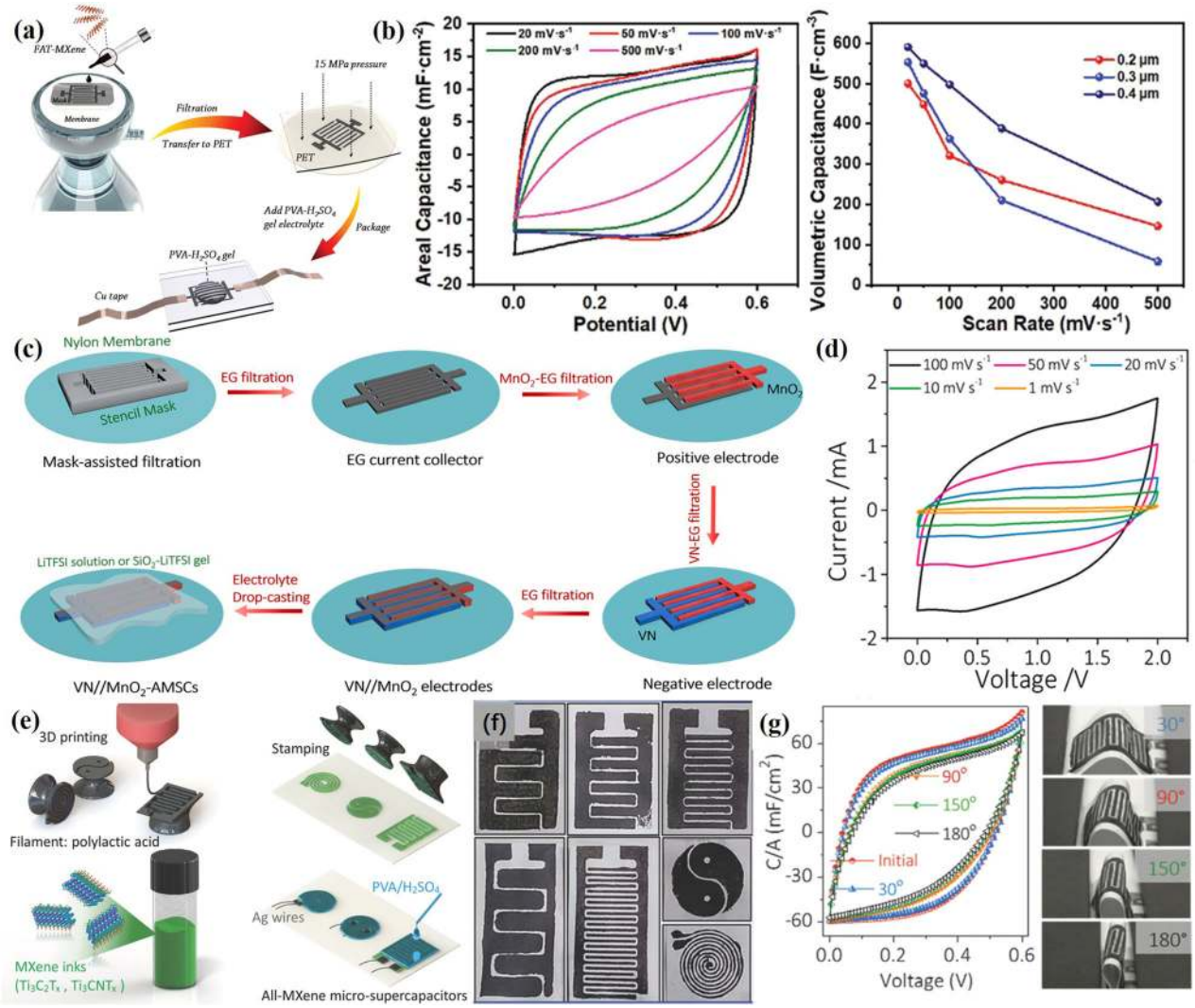

Fig. 4 Fabrication of MSCs by mask-assisted filtering and stamping. a The schematic diagram of the mask-assisted fabrication of all-MXene MSC. **b** CV curves at different scan rates (left) and the volumetric capacitances of the MSCs with different thicknesses (right). **c** Fabrication of VN//MnO_2-AMSCs by mask-assisted filtration. **d** CV curves measured at different scan rates of the device. **e** Fabrication process of all-MXene-based MSCs through the stamping strategy. **f** Photos of the MSCs with various architectures. **g** CV curves of as-stamped MSCs under different bended states. **a**, **b** Reproduced with permission[72] (Copyright © 2020, John Wiley and Sons). **c**, **d** Reproduced with permission[73] (Copyright © 2019, Elsevier). **e**–**g** Reproduced with permission[75] (Copyright © 2018, John Wiley and Sons).

fabricated. Similarly, Li et al.[78] first prepared MXene thin films by spin coating. Then, they developed titanium carbide-poly(3,4-ethylenedioxythiophene) (PEDOT) heterostructures by electrochemical deposition. And planar MSCs of such hybrid films were carved directly using an automated scalpel technique. In brief, the automated scalpel technology opens up possibilities in fabricating MSCs from coating technique-yielded films.

In a word, although there are a large variety of developed methods for manufacturing MSCs, each of them still has room for further improvements. Moreover, the exploration and research of various new methods will certainly enrich the category of preparation for MSCs and further promote its development.

DESIGN OF ELECTRODE MATERIALS

MSCs usually consist of four parts: electrodes, electrolyte, current collector and substrate. Electrodes are mainly used to provide adsorption sites for ions and electrons, either forming electric double layers or reacting chemically. And electrolyte mainly performs the function of transporting supplement ions to realize ionic conduction inside the circuit. The collector is the part that bridges the electrodes and outer wires, ensuring unblocked pathways for electrons shuttling between electrodes and external circuit. The substrate is used to carry the whole MSC device. Among them, electrode is the central component that largely affects the performance of MSCs[79]. At present, the commonly used electrode materials can be divided into three categories: carbon materials, metal-based materials and conducting polymers[80,81]. They have not only different properties but also distinct charge-storage mechanisms[82]. For the moment, rational selection and combination of different types of electrode materials that can make them fully functional to achieve better performance still remains a great challenge. Thus, in this section, we will compare and discuss the advantages and disadvantages of some typical and important electrode materials and propose reasonable solutions to their weakness. On the basis of this summary, useful guidelines for manufacturing high-performance MSCs will be defined.

Electric double-layer MSCs

Carbon materials are the most used electrodes for EDLCs owing to their large surface area, porosity and high compatibility with advanced manufacturing technologies of MSCs[83,84]. Based on dimensionality, carbon materials can be roughly classified into three types: zero-dimensional (0D) carbon materials including active carbon[85] and carbon/graphene dots[86], one-dimensional (1D) carbon materials including carbon nanotubes (CNTs) and carbon nanofibers[83,87], and two-dimensional (2D) carbon materials featured by graphene[62,88–91]. It is easy to envision the good rate capability and cyclic stability of carbon electrodes in view of aforementioned merits. However, the nature of electrostatic absorption mechanism largely limits their energy density. In this case, carbon materials with different dimensionalities have different remedies. For 0D and 1D carbon materials, the common strategy is to design porous nano/micro-structure to increase active sites. For example, Li et al.[92] used a solvent-free MOF-CVD method to coat interdigitated gold electrodes with a layer of nanoporous carbon as shown in Fig. 5a. Owing to the high porosity and conductivity of such MOF-derived porous carbon layer (Fig. 5b), the fabricated MSCs delivered a stack power of 232.8 W cm^{-3} at a high scan rate of 1000 mV s^{-1}. It is expected that other types of MOF materials can also produce nanoporous carbon electrodes by similar methods. It thus can provide some useful guidance for MSC fabrication. In addition to tuning the porosity, manipulating the arrangement of nano building blocks is another effective way toward high-capacitance carbon electrodes. For instance, Hsia et al.[87] prepared MSCs based on silicon wafer supported vertically aligned CNTs. The stability offered by the vertically aligned nanoarray could greatly suppress the overlapping of CNTs during electrode preparation process. Consequently, the enlarged effective contact area for electrolyte ions as well as increased active sites endowed the assembled MSC with improved energy density.

For 2D carbon materials such as graphene, a variety of strategies can be used to improve its electrochemical performance. Firstly, the main factor that restricts its high electrochemical performance is their re-stacking in the course of electrode preparation. To solve this problem, introduction of guest materials as spacers is proved to be feasible to prevent the stacking of 2D carbon materials. For example, Wang et al.[93] mixed graphene with CNTs to fabricate flexible MSCs. Owing to the presence of CNTs preventing the stacking of graphene (Fig. 5c, d), the as-prepared MSC exhibited a high areal energy density of 1.36 μWh cm^{-2} at 0.05 mA cm^{-2} and retained 95.5% of its capacitance after 10,000 cycles. In addition, creating in-plane pores allows graphene to increase performance by providing sufficient reactive sites and promoting the electrolyte ion diffusion. For example, Lu et al.[88] reported a MSC based on porous graphene yielded from electrochemical exfoliation and achieved a high areal capacitance of 6.41 mF cm^{-2} and exceptional mechanical flexibility. Besides above mentioned two strategies, atomic doping can not only improve the active sites but also the conductivity of electrode materials. Wu et al.[94] prepared a boron and nitrogen co-doped graphene (BNG) film through a layer-by-layer assembly method and then assembled it into a MSC, which delivered a ultrahigh volumetric capacitance (488 F cm^{-3}) and good rate capability (2000 mV s^{-1}). Such superior capacitive performance was a result of the synergistic effect of diatomic doping that could not only provide additional pseudo capacitance but also improve the wettability of graphene electrode.

In a word, carbon-based EDLCs have good rate capability and cycle stability. However, low capacitance and energy density limit their applications in some specific applications, such as integrated

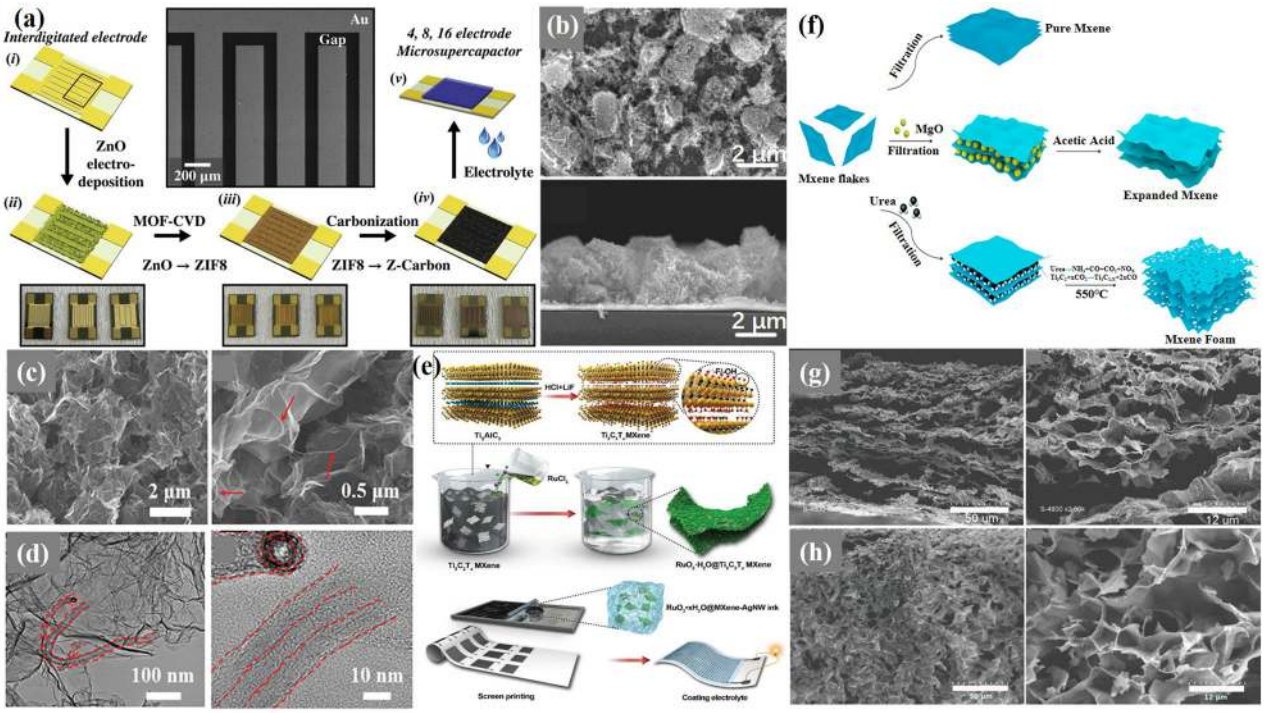

Fig. 5 Electrode materials optimization. a Schematic illustration of fabrication process for MSCs. **b** Top-view and cross-sectional SEM images of nanoporous carbon film. **c** Top view and **d** cross-sectional SEM images of graphene-CNT electrodes at different magnifications (the red part indicates the CNTs between graphene sheets). **e** Schematic illustration of the process for screen-printed $RuO_2{\cdot}xH_2O$@MXene–Ag NW nanocomposite ink-based MSCs. **f** Synthesis scheme of the preparation of various forms of MXene. Side views from SEM images of **g** expanded MXene and **h** Mxene foam. **a**, **b** Reproduced with permission[92] (Copyright © 2019, Elsevier). **c**, **d** Reproduced with permission[93] (Copyright © 2020, John Wiley and Sons). **e** Reproduced with permission[113] (Copyright © 2019, John Wiley and Sons). **f**–**h** Reproduced with permission[115] (Copyright © 2020, Elsevier).

systems requiring high capacitance. Even diverse measures (like pore forming, atom doping, etc.) have been taken to improve the capacitance and energy density, there is still a long way to explore higher performance carbon-based MSCs.

Pseudo MSCs

The pseudocapacitive materials usually contain conducting polymers (polyaniline, polypyrrole, polythiophenes)[69,95–100] and metal-based (Ru, Mn) compounds[76,101–105]. These materials store charge via fast and reversible faradic reactions providing higher capacitance than those EDLC materials. Especially, conducting polymers have shown great potential in MSCs because of their high conductivity, environmental friendliness and relatively low cost. Despite having such merits, MSCs based on conducting polymer still suffer from inferior cyclic stability and low energy density. It is a reasonable and effective method to promote the diffusion and permeation of electrolyte through reasonable structure design. For example, Zhu et al.[97] used electrochemical method to deposit Ppy nanowires with sac-like structure on a conductive glass. In this system, sac-like structures could promote the penetration of electrolyte, which was beneficial to enhance the electrochemical performance. In addition, this structure would shorten the diffusion distance of ions and solve the sluggish ion transportation to a certain extent. Therefore, the prepared MSCs with Ppy nanowires exhibited an ultrahigh energy density of 15.25 mWh cm^{-3} at a high power density of 0.89 W cm^{-3}.

Currently, metal-based materials have been widely studied in the field of electrochemical energy storage because of their high theoretical capacity and abundant reserves. However, due to their poor conductivity and low cycle performance, the application of these materials is limited. An effective strategy is to improve the electrical conductivity of metal-based materials by doping atoms, so as to further improve their electrochemical performance. For example, Wang et al.[50] used a simple bottom-up method to displace and dope three-dimensional metal ions (Co, Fe, Ni) into two-dimensional MnO_2 nanosheets. In this system, the 3d metal ions not only introduced new electronic states near the Fermi level but also improved the electronic conductivity. Therefore, the fabricated MSCs with Fe-doped MnO_2 nanosheets on polyimide substrates showed a high volumetric energy density of up to 1.13×10^{-3} Wh cm^{-3} at a power density of 0.11 W cm^{-3} and excellent mechanical properties. Another effective strategy is to promote the penetration and diffusion of electrolyte ions by reasonable structure and morphology design similar to the optimization of carbon-based materials. For example, Lei et al.[106] prepared a microminiaturized honeycomb alumina nanoscaffold. Based on this structure, high performance MSCs with a capacitance of 128 mF cm^{-2} at 0.5 mA cm^{-2} was prepared. Because this structure could provide a stable platform for the active materials of micro supercapacitors. In this kind of vertical arrangement structure, enough active area of electrode could be provided and effective ion migration could be achieved.

It is worth mentioning that, as a new class of 2D metal compounds in the field of electrochemistry, MXene has attracted wide attention in planar MSCs because its 2D open structure can offer high surface area, good electron mobility, as well as excellent electrolyte permeability[107–110]. However, like graphene, 2D MXene sheets also endure severe re-stacking in practical application[111,112]. Therefore, it is necessary to take steps avoiding its re-stacking prior to real use. As shown in Fig. 5e, Li et al.[113] employed RuO_2 nanoparticles as spacers to expand the MXene sheets, and then mixed with silver nanowire (AgNW) to fabricate MSCs. Owing to the spacing effect of RuO_2 nanoparticles resulting in effective ion channels, the prepared MSC showed high volumetric capacitances of 864.2 F cm^{-3} at 1 mV s^{-1} and 304.0 F cm^{-3} at 2000 mV s^{-1}. It also showed long-term cycling performance of 90% retention after 10,000 cycles and outstanding flexibility. Similarly, Chen et al.[114] introduced MoS_2 into MXene and assembled them into symmetrical MSCs. It should be pointed out that the adoption of MoS_2 could not only inhibit the restacking of MXene sheets but also contribute extra pseudocapacitance by virtue of its pseudocapacitive nature. Consequently, the fabricated MSC exhibited high specific capacitance of 173.6 F cm^{-3} and energy density of 15.5 mWh cm^{-3}. In addition, as shown in Fig. 5f, Zhu et al.[115] developed two efficient methods to prevent MXene layers from aggregation by enlarging the interlayer spacing with foreign materials and creating in-plane pores (Fig. 5g, h). As a result, the electrochemically active area and ion transport efficiency were greatly improved, leading thus to much augmented capacitive performance. Table 1 compares the performance of MSCs made by different methods and electrode materials. It can be seen that pseudo-MSCs generally have higher capacitance than EDLCs. However, new strategies are still highly desired to develop MSCs with both high capacitance and good cycle stability.

Asymmetric MSCs

As mentioned above, MSC devices assembled from EDL or pseudo-capacitor materials alone are hard to have high energy density, power density and good cyclic stability at the same time. In this case, it holds great potential to combine two types of materials together and unify their respective advantages to obtain superior asymmetric MSC devices[116,117]. One strategy is to make capacitive asymmetric MSCs with both EDLC and pseudo-capacitor materials. For example, Liu et al.[118] reported an asymmetric MSC using nitrogen-doped graphene quantum dots (N-GQDs) as negative electrode and molybdenum disulfide quantum dots (MoS_2-QDs) as positive electrode, and achieved a large operating voltage up to 1.5 V and a high energy density of 0.55 mWh cm^{-3}. In addition, Gao et al.[61] prepared an integrated MSC array based on MnO_2@Ppy@MWCNT (multiwalled carbon nanotube) anode and Ppy@MWCNT cathode. The MWCNT could provide large active surface area and efficient electron transfer channel, while MnO_2 and Ppy were beneficial to improve the capacitance. As a result, the MSC array could output a voltage of as high as 9.6 V. Furthermore, using two types of 2D materials to prepare asymmetric MSCs has been demonstrated. Couly et al.[119] fabricated a high-performance MSC on a flexible substrate by utilizing MXene and reduced graphene oxide (rGO) as positive and negative electrode materials, respectively. Benefiting from the features (large surface area, rapid ion diffusion, etc.) of 2D materials, the flexible MSC exhibited an energy density of 8.6 mWh cm^{-3} at 0.2 W cm^{-3} and a wide voltage window of 1 V.

Another strategy is to build hybrid MSCs, where one electrode has capacitive charge-storage mechanism and another has battery-type Faradaic mechanism. By reason of the battery-type electrode providing high capacitance and effectively expanding the working voltage window, the hybrid MSCs can gain higher energy density than the symmetric MSCs counterpart.[120] For example, Zhang et al.[121] reported a Zn-ion hybrid MSC based on Zn-nanosheet anode and activated carbon cathode. Because of complementary advantages of capacitor-type and battery-type materials, the prepared MSC showed excellent areal energy density of 115.4 μWh cm^{-2} at 0.16 mW cm^{-2}.

In a word, asymmetric MSCs have broad prospects as they possess not only high capacitance and power density, but also good cyclic stability. This enables them to satisfy many complex application scenarios. In particular, hybrid MSCs can obtain wider voltage window and higher energy density than symmetric MSCs by using both battery-type and capacitive materials simultaneously. Even so, ingenious design and optimization of electrode materials are still needed to obtain MSCs with higher energy density.

Table 1. Performance of MSCs with different methods and electrode materials.

Method	Electrode materials	Capacitance	Energy density	Power density	Capacitance cycle stability	Ref.
Screen printing	Graphene/CNTs	7.7 mF cm^{-2} 77.3 F cm^{-3}	10.7 mWh cm^{-3}	3.17 W cm^{-3}	<1% loss after 15,000 cycles	30
Screen printing	Ag@Ppy	576.6 F g^{-1} 47.5 mF cm^{-2}	4.33 μWh cm^{-2}	0.6 mW cm^{-2}	17.4% loss after 10,000 cycles	39
Screen printing	MXene	158 mF cm^{-2}	1.64 μWh cm^{-2}	778.3 μW cm^{-2}	4.2% loss after 17,000 cycles	41
Screen printing	RuO_2·xH_2O@MXene–AgNW	864.2 F cm^{-3}	13.5 mWh cm^{-3}	48.5 W cm^{-3}	10% loss after 10,000 cycles	113
Inkjet printing	Fe-doped MnO_2	1.2 mF cm^{-2} 9.2 F cm^{-3}	1.13 mWh cm^{-3}	0.11 W cm^{-3}	21.3% loss after 5200 cycles	50
Inkjet printing	MnO_2/Ag	125.76 F g^{-1}	17.5 Wh kg^{-1}	500.95 W kg^{-1}	9% loss after 1000 cycles	52
Inkjet printing	MXene	12 mF cm^{-2}	0.32 μWh cm^{-2}	158 μW cm^{-2}	No capacitance loss after 10,000 cycles	49
Photolithography	SWNT/carbon/MnO_2	550 μF cm^{-2} 20.4 F cm^{-3}	–	–	7.6% loss after 5000 cycles	57
Photolithography	C/Sn QDs	5.79 mF cm^{-2} 22.44 F cm^{-3}	–	–	6.7% loss after 5000 cycles	58
Photolithography	Holey graphene/polyaniline	271.1 F cm^{-3}	24.1 mW h cm^{-3}	110.1 W cm^{-3}	0.5% loss after 5000 cycles	59
Laser scribing	LIG	0.62 mF cm^{-2}	0.92 μWh cm^{-2}	~290 μW cm^{-2}	No capacitance loss after 10,000 cycles	66
Laser scribing	B-doped LIG	16.5 mF cm^{-2} 6.6 F cm^{-3}	0.74 mWh cm^{-3}	~4.7 W cm^{-3}	10% loss after 12,000 cycles	65
Laser scribing	RuO_2/Au	27 mF cm^{-2} 540 F cm^{-3}	3.1 μWh cm^{-2}	~2.3 mW cm^{-2}	20% loss after 10,000 cycles	68
Mask-assisted filtering	Phosphorene/graphene	9.8 mF cm^{-2} 37.0 F cm^{-3}	11.6 mWh cm^{-3}	1500 mW cm^{-3}	10.5% loss after 2000 cycles	70
Mask-assisted filtering	FAT-MXene	23.6 mF cm^{-2} 591 F cm^{-3}	29.6 mWh cm^{-3}	18.6 W cm^{-3}	2.2% loss after 2000 cycles	72
Stamping	MXene	61 mF cm^{-2}	0.76 μWh cm^{-2}	0.33 mW cm^{-2}	5.9% loss after 10,000 cycles	75
Pencil-drawing	MnO_2/graphite	40.2 mF cm^{-2}	–	–	14.2% loss after 2000 cycles	76
Dip coating/scalpel	MXene	283 μF cm^{-2}	~0.012 μWh cm^{-2}	~ 101 μW cm^{-2}	~ 2% loss after 6000 cycles	77
Spray coating/scalpel	PEDOT/$Ti_3C_2T_X$	2.4 mF cm^{-2}	8.7 mWh cm^{-3}	4.5 W cm^{-3}	10% loss after 10,000 cycles	78
Direct ink writing	Graphene-CNT	9.81 mF cm^{-2}	1.36 μWh cm^{-2}	0.25 mW cm^{-2}	4.5% loss after 10,000 cycles	93

~approximated from Ragone plots in the literature.

APPLICATION OF MSCS

The continuing growth of microelectronic systems requires the progress of small energy storage devices[122]. And MSC can well meet the increasing requirements of highly integrated and flexible electronics owing to its small-size, lightweight, extremely high charge/discharge rate, as well as high flexibility. Till now, they have already been effectively applied to advanced wearable devices, various types of sensors, and so on[123]. Moreover, they can play an important role in medicine-related area because of the selection diversity of electrode materials. In this section, we will summarize the applications of MSCs in representative electronic devices, focusing on their complementary roles to make these devices function.

Energy storage

In recent years, the sustained development of wearable electronic devices and various types of small sensors have greatly stimulated the demand for corresponding power supply modules[124]. However, for the moment, the main difficulty resides in obtaining stable and long-term continuous power supply modules. The limited service life of micro-batteries and working conditions of solar cells (only with illumination) cannot meet this requirement. In this case, connecting MSCs with energy harvest devices (e.g., triboelectric nanogenerator) is an attractive solution to fulfill this requirement. For example, Luo et al.[125] developed a simple laser engraving technology to integrate MSCs with TENG to form a self-powered system. The system could complete the charging process by simple mechanical movement, and had excellent continuous discharge ability. However, it usually took a long time to charge MSCs in similar systems to support practical application. To solve this problem, Zhang et al.[126] put forward a strategy by employing dual energy harvest devices, e.g. electromagnetic generators (EMG) and TENG, to collect the mechanical energy (Fig. 6a), which greatly increased the charging rate of MSCs. And the whole system was integrated in a bracelet and could be easily worn on the wrist. From that, the MSCs could be charged to 2 V only by swinging the wrist in daily action, which could support the use of multiple sensors. In addition, MXene-based MSCs also show good potential in self-powered systems. As shown in Fig. 6b, Jiang et al.[127] built a highly compact self-charging power module via integrating the triboelectric nanogenerator (TENG) and MXene-MSC. Such an integration unit could be harmlessly worn on human skin and converted the mechanical energy generated by human motion into electrical energy and store it in MSC. Note that the powered MSC can be further used to drive a variety of electronic wearable sensors. In conclusion, connecting flexible MSCs as energy storage devices with energy harvest devices can continuously supply energy for small integrated systems for a long time regardless of the external conditions. This can further improve the possibility of practical application of wearable electronic devices.

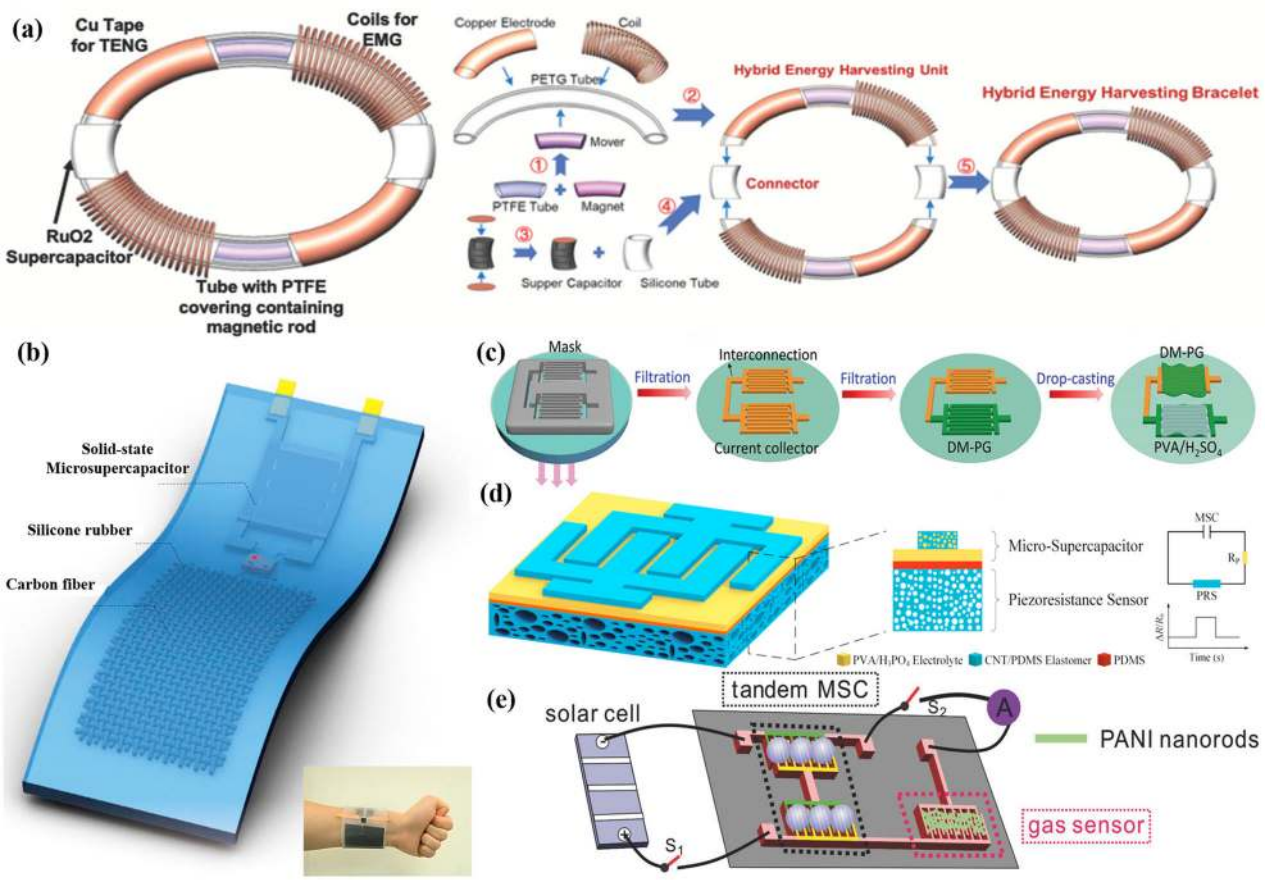

Fig. 6 MSCs for energy storage and sensors integration. a The fabrication process of the hybrid energy harvesting bracelet. **b** Schematic diagram of the wearable self-charging system device, inset photograph demonstrates that the system worn on the forearm. **c** Fabrication of the planar MSC-sensor integrated system. **d** Schematic illustration of all-in-one sensing patch based on the porous CNT-PDMS elastomer. **e** Schematic of the self-powered integrated device. **a** Reproduced with permission[126] (Copyright © 2019, John Wiley and Sons). **b** Reproduced with permission[127] (Copyright © 2018, Elsevier). **c** Reproduced with permission[131] (Copyright © 2020, John Wiley and Sons). **d** Reproduced with permission[132] (Copyright © 2018, Elsevier). **e** Reproduced with permission[135] (Copyright © 2017, John Wiley and Sons).

Integration with various types of sensors

As mentioned above, MSCs can be used to power various types of sensors, and their integration can be applied in many fields[128,129]. For example, MSCs coupled with gas sensor can monitor the change of surrounding gas in real time, which is of great significance to control environmental quality and human health. Yun et al.[130] reported a MSC-gas sensor system, where the gas sensor consisted of graphene and the MSCs were made from polyaniline-wrapped MWCNTs. Through the rational design of the substrate, the two devices could be effectively integrated together and showed excellent tensile property of a uniaxial strain of 50% without electrochemical performance changing. Moreover, this system could test NO_2 gas for longer than 50 min, suggesting an efficient integration of these two devices. Nevertheless, it is found that different cells use different active materials, which may not only complicate the material manufacturing but also reduce the compatibility of different modules. In this context, it is highly desirable to construct multifunctional materials that can work for all the devices involved. For instance, Qin et al.[131] reported the synthesis of 2D hierarchically ordered dual-mesoporous Ppy/graphene (DM-PG) nanosheets as bi-functional active materials for both MSC and NH_3 sensor (Fig. 6c). Owing to the sharing of the same active material, the fabricated MSC-sensor system had high compatibility and could respond exposed to 10–40 ppm of NH_3 only after being charged for 100 s. More importantly, in the case of large bending, it still had a good response value for NH_3.

Except gas sensor, Song et al.[132] also reported the assembly of the piezoelectric sensors (PRSs) and MSC, enabling the real-time pressure detection. As shown in Fig. 6d, through solution-evaporation method, an all-in-one sensing patch consisted of PRS as functional fraction and MSC built from porous CNT-polydimethylsiloxane (CNT-PDMS) elastomer as energy storage fraction was successfully packaged. It should be noted that both the sensor and MSC worked well after integration. The PRS had high sensitivity of 0.51 kPa^{-1} and wide detection range while MSC showed excellent areal capacitance. What's more, the prepared patch could be easily attached to human skin to detect body condition. And it also could be utilized as a 3D touch, we could extract its characteristic parameters and interpret signals for user identification and so on. In addition, the integrated system of MSCs for strain sensor has also been successfully prepared. By integrating MSCs, solar cells and strain sensors, Yun et al.[133] made a self-powered system to drive the sensors to work. The system had excellent tensile properties and could detect the change of external strain.

Moreover, through the integration of MSCs and UV sensor, one can realize the UV detection. For example, Kim et al.[134] fabricated an all-solid-state flexible MSCs array based on graphene foam/MWCNT-COOH/MnO_x. After being coupled with SnO_2 nanowire-based UV sensor, the system could directly measure the UV-induced photocurrent and the response time could exceed 10 min. Through further integration with solar cells, the sensor

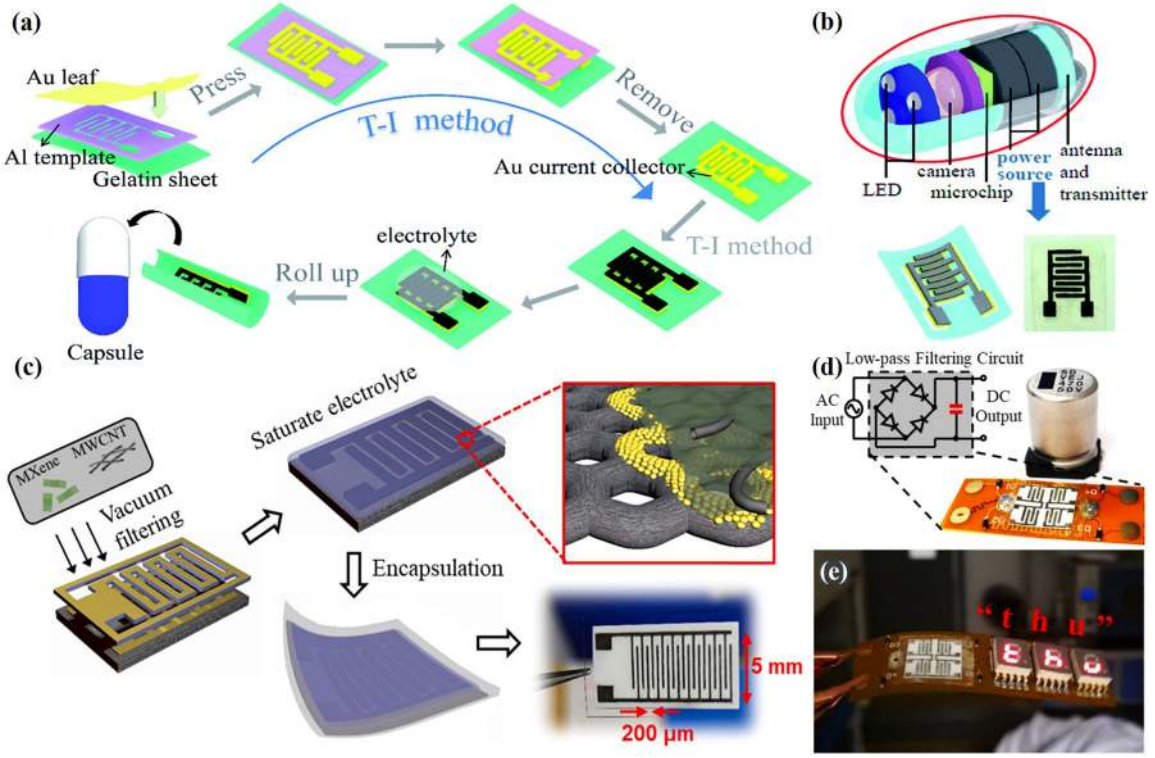

Fig. 7 Applications of MSCs in medical assistant and AC line-filtering. a The schematic illustration of fabrication of EMSC. **b** Structure diagram of commercial gastroscope powered by the EMSC. **c** Schematic diagram showing the fabrication process of high-frequency MSC. **d** Circuit diagram and photograph of a low-pass filtering circuit. An electrolytic capacitor of 0.47 mF is shown for comparison. **e** A LED array is powered through flexible power filtering circuit with AC input. **a**, **b** Reproduced with permission[137] (Copyright © 2020, Royal Society of Chemistry). **c**–**e** Reproduced with permission[141] (Copyright © 2019, Elsevier).

system could be self-powered. Guo et al.[135] reported a strategy to integrate nanowires-based UV sensor and MSCs on a piece of paper with printing Ni circuit. The resulting MSC-UV sensor system showed good sensing and self-powering capabilities. And they also prepared a gas sensor system with the MSC charged by connecting with a solar cell. Corresponding schematic diagram is shown in Fig. 6e. Similarly, Cai et al.[136] demonstrated a self-powered UV-light detection system through combining a MSC produced by laser direct writing on PI films, a ZnO nanoparticles-based photodetector also made by one-step laser direct writing and a solar panel. As a result, the system had fast response ability and high on/off ratio.

In short, micro sensor integrated systems play an increasingly important role in monitoring environmental, gas, and so on. In most cases, these systems must have certain flexibility to adapt to various application scenarios, such as sticking to human skin. And the further development of sensor integrated system needs the support and prop up from the MSCs with superior flexibility, high power density, fast charging rate and response time.

Medical assistant examination

The rapid growth of painless diagnosis demand promotes the miniaturization of medical devices. Due to the uncertainty of the pathological characteristics of most biocompatible materials, and the discontinuity of electrode elements under the complex and variable surface strain, new degradable energy devices often show unpredictable performance and huge safety risks in the diagnosis process. In this case, because of its small size, good flexibility and strong selectivity of electrode materials, MSCs provide an opportunity for the application of medical auxiliary energy. For example, inspired by the electrochemical behaviors of natural food, Gao et al.[137] developed an edible MSC (EMSC) made from food constituents by template-imprinting strategy, with the production process shown in Fig. 7a. In this structure, the involved electrode and electrolyte materials were non-toxic and harmless and could be absorbed or degraded by human body. The fabricated EMSC exhibited excellent mechanical stability and flexibility, enabling the attachment of it to the objects of various shapes, such as human skin and fruit. Moreover, this micro-device could be coiled into a shell of medical capsule to provide power supply for capsule endoscopy in simulated gastric juice environment as shown in Fig. 7b. The prominent properties of the MSCs pave the way toward real-time vivo detection and other biological application possibilities.

Another kind of important wearable electronic devices for personal health is flexible and attachable body fluid monitoring smart system, which can predict health status in real-time by monitoring the composition of body fluids. Because of the flexibility and selectivity of the substrate, the planar MSCs can meet this demand. For example, Lu et al.[138] prepared a perspiration monitoring system with the integration of $NiCo_2O_4$-based MSC. The as-fabricated MSC displayed an energy density of 0.64 μW cm^{-2}. Moreover, the designed system displayed excellent monitoring performance and sensitivities for ions and glucose in sweat. More interestingly, this system could be combined with wireless sensor technology to achieve real-time monitoring of sweat accurately, and could send relevant information to the mobile phone for health assessment. In short, flexible MSCs can avoid the frequent replacement problem that micro-batteries always face due to their short lifespan. Moreover, the biodegradable materials-derived MSCs are capable of causing no harm to organisms. All in all, the rational use of MSCs is expected to further promote the progress and development of area of medicine.

Alternating current (AC) line-filtering

Aluminum electrolytic capacitors (AECs) are widely used for AC line-filtering applications. However, AECs normally have large volume but low volumetric energy density, which is incompatible to the development of intelligent devices, especially on-chip technology[139]. In contrast to AECs, MSCs are small in size, easy to integrate and have high power density, rendering them suitable for AC line-filtering. Yang et al.[140] fabricated a MSC based on an azulene-bridged coordination polymer framework through a layer-by-layer method. The prepared MSC had specific capacitances of up to 34.1 F cm^{-3} at 50 mV s^{-1} and reached a phase angle of −73° at 120 Hz with a short resistance-capacitance constant of circa 0.83 ms. Whereas at present, unsatisfied rate capability still remains a bottleneck limiting the application of MSCs in filtering field. To address this issue, MXene and graphene are regarded as well-suited candidates owing to their multiple ionic channels and fast surface redox reactions. For example, Xu et al.[141] reported a high-frequency MSC based on hybrid architecture electrode consisting of 2D pseudocapacitive MXene and MWCNTs, as shown in the Fig. 7c. Since MXene provided high capacitance as active material and MWCNT offered fast ion transport pathways as interlayer support, the resulting MSC exhibited high power density and a better frequency response than commercial tantalum capacitors at 120 Hz. Moreover, the MSC showed superior performance in both low-pass filter circuit and a relaxation oscillator circuit to electrolytic capacitors in terms of function and size (Fig. 7d). And as shown in Fig. 7e, this system could supply power to LED array successfully under AC voltage. Likewise, Jiang et al.[142] also assembled a MSC based on solution processable 2D MXene nanosheets and successfully applied it on AC line-filtering. Through optimizing the flake size, thickness of the electrodes, and spacing between the electrode fingers, the as-prepared MSC delivered a volumetric capacitance of 30 F cm^{-3} at 120 Hz and had a relaxation time constant of $\tau_0 = 0.45$ ms, which was better than electrolytic capacitors ($\tau_0 = 0.8$ ms). Therefore, the device could filter 120 Hz ripples.

In short, compared with AECs, MSCs with unique advantages exhibit tremendous potential for AC line-filters for electronic devices and Internet of Things (IoTs).

SUMMARY AND OUTLOOK

In conclusion, this review introduces the research progress of MSCs in structure design, manufacturing methods, electrode materials, and main applications areas. In recent years, the research of MSCs has made encouraging progress. In the following, our opinions on the main developments and challenges of planar MSCs are provided.

(1) In terms of device structure, compared with the traditional sandwich structure, the interdigital structure has obvious advantages, that is to say, it can not only greatly shorten the ion diffusion distance, but also enable the diverse integrations of MSCs with other devices. Note that the mechanical properties of interdigital MSCs have also achieved great accomplishments. In order to adapt to complex application conditions, flexible MSCs with excellent bending, tensile and even torsional properties have been reported one after another. These good mechanical properties are mainly issued from the flexibility of substrates. At present, the commonly used flexible substrates are PET, PI, paper and so on. However, the flexibility of MSC devices inherited from these substrates seems to be a little insufficient to keep pace with the rapid development of flexible integrated systems. Therefore, to meet the ever-demanding standards for wearable devices and intelligent integrated systems, people set higher and higher requirements to the mechanical properties of flexible MSC devices. Although developing more flexible, lighter substrates represents an effective approach to realize the high flexibility of MSCs, it may take a lot of time and effort. Alternatively, one can design the patterns and microstructures of electrode materials with superstructure shapes by cutting the substrates and electrode material films directly with the help of laser and templates. Recently, flexible MSC arrays with Kirigami superstructures have been fabricated by laser cutting active material films and show excellent tensile properties, remaining stable even at the stretching of up to 200% elongation[31,143]. However, there are few reports on flexible MSCs with other superstructures, like origami, etc. Therefore, improving the mechanical properties of flexible MSCs would be a hopeful direction to accommodate with different specific requirements.

(2) In terms of device manufacturing, the micro machining technologies of MSCs have made great progress. It should be noted that each emerging production method comes with its own advantages and disadvantages. To be specific, screen printing process is simple and highly efficient owing to the fact that electrode materials and electrolyte can be simultaneously printed to make all-printed solid-state (or quasi-solid-state) MSCs. This also makes it possible to realize the mass production of MSCs. However, screen printing needs to obtain device pattern with the help of a mask, of which the resolution is not high. Moreover, it is also necessary to prepare ink with good fluidity to avoid the jam of the screen. Compared with screen printing, inkjet printing omits the use of masks, but cannot avoid the jam problem. By contrast, photolithography can produce MSCs with high precision and resolution in nanometer size. But it requires a multi-step manufacturing process and an ultraclean working environment, which severely limits its further development. As a new micromachining method with simple process and flexible operation, laser scribing shows great potential in MSCs manufacturing. This is because it can not only produce electrode materials by laser irradiating special precursor, but also directly cut materials or substrates into high-precision pattern. For the mask-assisted filtering method, despite of the need of pre-fabricated mask with required patterns, it still deserves a place in MSCs manufacturing by virtue of its simple operation and strong universality. Besides these technologies, 3D printing is capable of making high-precision 3D electrode materials with excellent electrochemical performance. And, given that, it is of high possibility that 3D printing may become a key technology for the future production of on-chip MSCs.

(3) In terms of electrode materials, excellent electrode materials are the key to realize high performance MSCs. Advanced 2D materials such as graphene and MXene are considered to be promising electrode materials because their 2D open structures can provide high active surface area and abundant ion diffusion channels. In addition, some conducting polymers such as Ppy and metal-based materials such as RuO_2 are also potential electrode materials because they can provide high capacitance. It also should be noted that high energy density has always been the goal pursued by MSCs devices. To this end, constructing active materials with high conductivity and multiple ion diffusion channels by introducing heteroatoms or pores is proved to be quite efficient. Note that advanced micro machining technologies (like laser scribing, screen printing, etc.) allow easy implementation of porous or hetero-structure into electrode materials. In addition to modifying the electrodes intrinsically, it is also quite effective to increase the energy density of MSCs by hybridizing the EDLC materials and pseudo-capacitive or battery-type materials to build asymmetric MSCs. The yielded hybrid MSCs are able to work in a wide voltage range and achieve high energy density. However, the quest of high-performance planar MSCs never stops, and challenges still remain to meet such ever-increasing demands.

(4) In terms of the applications of MSCs, various integration and functional systems have employed MSCs as an indispensable part. For most functional energy harvesters, they are still in the primary

stage of concept exhibition and experimental research, and not really applied yet. The key now is to improve the compatibility of MSCs with energy collection devices to improve energy conversion efficiency. In addition, MSCs can also be integrated with a variety of sensors and thus have different functions depending on the types of the sensors, such as gas sensors, pressure sensors. In such an assembling system, how to increase the sensitivity of the sensor and the matching degree between the sensor and MSCs remains a core topic. Moreover, reducing the volume of the integrated system up to the hilt to meet the needs of different scenarios is also challenging. For medical assistant equipment, it is quite promising to develop non-toxic and harmless MSCs materials that are easy to absorb or decompose. And for AC line-filter, the electrochemical performance and filtering ability can be further developed by increasing the speed capability and capacitance capacity of MSCs. It is worth noting that the MSCs have a broad prospect in applications.

DATA AVAILABILTY

All data are available within the article or available from the authors upon reasonable request.

Received: 20 June 2020; Accepted: 10 October 2020;
Published online: 16 November 2020

REFERENCES

1. González, A., Goikolea, E., Barrena, J. A. & Mysyk, R. Review on supercapacitors: technologies and materials. *Renew. Sust. Energ. Rev.* **58**, 1189–1206 (2016).
2. Chen, D., Lou, Z., Jiang, K. & Shen, G. Device configurations and future prospects of flexible/stretchable lithium-ion batteries. *Adv. Funct. Mater.* **28**, 1805596 (2018).
3. Wang, Y. & Xia, Y. Recent progress in supercapacitors: from materials design to system construction. *Adv. Mater.* **25**, 5336–5342 (2013).
4. Kyerematen, N. A., Brousse, T. & Pech, D. Microsupercapacitors as miniaturized energy-storage components for on-chip electronics. *Nat. Nanotechnol.* **12**, 7–15 (2017).
5. García Núñez, C., Manjakkal, L. & Dahiya, R. Energy autonomous electronic skin. *npj Flex. Electron.* **3**, 1 (2019).
6. Wang, Y., Cao, Q., Guan, C. & Cheng, C. Recent advances on self-supported arrayed bifunctional oxygen electrocatalysts for flexible solid-state Zn-air batteries. *Small* **16**, 2002902 (2020).
7. Liu, N. & Gao, Y. Recent progress in micro-supercapacitors with in-plane interdigital electrode architecture. *Small* **13**, 1701989 (2017).
8. Wang, J., Li, F., Zhu, F. & Schmidt, O. G. Recent progress in micro-supercapacitor design, integration, and functionalization. *Small Methods* **3**, 1800367 (2018).
9. Yue, C. et al. High stability induced by the TiN/Ti interlayer in three-dimensional Si/Ge nanorod arrays as anode in micro lithium ion battery. *ACS Appl. Mater. Interfaces* **8**, 7806–7810 (2016).
10. Liu, L. et al. Advances on microsized on-chip lithium-ion batteries. *Small* **13**, 1701847 (2017).
11. Ren, J. et al. Twisting carbon nanotube fibers for both wire-shaped micro-supercapacitor and micro-battery. *Adv. Mater.* **25**, 1155–1159 (2013).
12. Salian, G. D. et al. Niobium alloying of self-organized TiO_2 nanotubes as an anode for lithium-ion microbatteries. *Adv. Mater. Technol.* **3**, 1700274 (2018).
13. Liu, L., Niu, Z. & Chen, J. Design and integration of flexible planar micro-supercapacitors. *Nano Res.* **10**, 1524–1544 (2017).
14. Hu, H., Pei, Z. & Ye, C. Recent advances in designing and fabrication of planar micro-supercapacitors for on-chip energy storage. *Energy Storage Mater.* **1**, 82–102 (2015).
15. El-Kady, M. F. & Kaner, R. B. Scalable fabrication of high-power graphene micro-supercapacitors for flexible and on-chip energy storage. *Nat. Commun.* **4**, 1475 (2013).
16. Li, Z. et al. Nitrogen and oxygen co-doped graphene quantum dots with high capacitance performance for micro-supercapacitors. *Carbon* **139**, 67–75 (2018).
17. Qi, D., Liu, Y., Liu, Z., Zhang, L. & Chen, X. Design of architectures and materials in in-plane micro-supercapacitors: current status and future challenges. *Adv. Mater.* **29**, 1602802 (2017).
18. Yoo, J., Byun, S., Lee, C.-W., Yoo, C.-Y. & Yu, J. Precisely geometry controlled microsupercapacitors for ultrahigh areal capacitance, volumetric capacitance, and energy density. *Chem. Mater.* **30**, 3979–3990 (2018).
19. Pech, D. et al. Influence of the configuration in planar interdigitated electrochemical micro-capacitors. *J. Power Sources* **230**, 230–235 (2013).
20. Shi, X. et al. Graphene-based linear tandem micro-supercapacitors with metal-free current collectors and high-voltage output. *Adv. Mater.* **29**, 1703034 (2017).
21. Mirvakili, S. M. & Hunter, I. W. Vertically aligned niobium nanowire arrays for fast-charging micro-supercapacitors. *Adv. Mater.* **29**, 1700671 (2017).
22. Han, J. et al. On-chip micro-pseudocapacitors for ultrahigh energy and power delivery. *Adv. Sci.* **2**, 1500067 (2015).
23. Li, X., Yang, X., Xue, H., Pang, H. & Xu, Q. Metal–organic frameworks as a platform for clean energy applications. *EnergyChem* **2**, 100027 (2020).
24. Shi, X. et al. Ultrahigh-voltage integrated micro-supercapacitors with designable shapes and superior flexibility. *Energ. Environ. Sci.* **12**, 1534–1541 (2019).
25. Zhang, J., Zhang, G., Zhou, T. & Sun, S. Recent developments of planar micro-supercapacitors: fabrication, properties, and applications. *Adv. Funct. Mater.* **30**, 1910000 (2020).
26. Li, H. & Liang, J. Recent development of printed micro-supercapacitors: printable materials, printing technologies, and perspectives. *Adv. Mater.* **32**, 1805864 (2020).
27. Mendoza-Sanchez, B. & Gogotsi, Y. Synthesis of two-dimensional materials for capacitive energy storage. *Adv. Mater.* **28**, 6104–6135 (2016).
28. Beidaghi, M. & Gogotsi, Y. Capacitive energy storage in micro-scale devices: recent advances in design and fabrication of micro-supercapacitors. *Energ. Environ. Sci.* **7**, 867–884 (2014).
29. Li, J. et al. Scalable fabrication and integration of graphene micro-supercapacitors through full inkjet printing. *ACS Nano* **11**, 8249–8256 (2017).
30. Chih, J.-K., Jamaluddin, A., Chen, F., Chang, J.-K. & Su, C.-Y. High energy density of all screen-printable solid-state microsupercapacitor integrated by graphene/CNTs as hierarchical electrodes. *J. Mater. Chem. A* **7**, 12779–12789 (2019).
31. Jiao, S., Zhou, A., Wu, M. & Hu, H. Kirigami patterning of MXene/bacterial cellulose composite paper for all-solid-state stretchable micro-supercapacitor arrays. *Adv. Sci.* **6**, 1900529 (2019).
32. Zhao, X., Zhang, Y., Wang, Y. & Wei, H. Battery-type electrode materials for sodium-ion capacitors. *Batteries Supercaps* **2**, 1–20 (2019).
33. Mei, B.-A., Munteshari, O., Lau, J., Dunn, B. & Pilon, L. Physical interpretations of Nyquist plots for EDLC electrodes and devices. *J. Phys. Chem. C.* **122**, 194–206 (2017).
34. Borenstein, A. et al. Carbon-based composite materials for supercapacitor electrodes: a review. *J. Mater. Chem. A* **5**, 12653–12672 (2017).
35. Da, Y. et al. Engineering 2D architectures toward high-performance micro-supercapacitors. *Adv. Mater.* **31**, 1802793 (2019).
36. Das, P., Shi, X., Fu, Q. & Wu, Z. S. Substrate-free and shapeless planar micro-supercapacitors. *Adv. Funct. Mater.* **30**, 1908758 (2019).
37. Liang, J., Tian, B., Li, S., Jiang, C. & Wu, W. All-printed MnHCF-MnO_X-based high-performance flexible supercapacitors. *Adv. Energy Mater.* **10**, 2000022 (2020).
38. Li, W., Yang, S. & Shamim, A. Screen printing of silver nanowires: balancing conductivity with transparency while maintaining flexibility and stretchability. *npj Flex. Electron.* **3**, 13 (2019).
39. Liu, L. et al. All-printed solid-state microsupercapacitors derived from self-template synthesis of Ag@PPy nanocomposites. *Adv. Mater. Technol.* **3**, 1700206 (2018).
40. Yu, L. et al. Versatile N-doped MXene ink for printed electrochemical energy storage application. *Adv. Energy Mater.* **9**, 1901839 (2019).
41. Abdolhosseinzadeh, S. et al. Turning trash into treasure: additive free MXene sediment inks for screen-printed micro-supercapacitors. *Adv. Mater.* **32**, 2000716 (2020).
42. Singh, M., Haverinen, H. M., Dhagat, P. & Jabbour, G. E. Inkjet printing-process and its applications. *Adv. Mater.* **22**, 673–685 (2010).
43. Li, J. et al. Efficient inkjet printing of graphene. *Adv. Mater.* **25**, 3985–3992 (2013).
44. Wang, S. et al. Inkjet printing of conductive patterns and supercapacitors using a multi-walled carbon nanotube/Ag nanoparticle based ink. *J. Mater. Chem. A* **3**, 2407–2413 (2015).
45. Li, X. et al. Layer-by-layer inkjet printing GO film anchored $Ni(OH)_2$ nanoflakes for high-performance supercapacitors. *Chem. Eng. J.* **375**, 121988 (2019).
46. Hyun, W. J. et al. Scalable, self-aligned printing of flexible graphene micro-supercapacitors. *Adv. Energy Mater.* **7**, 1700285 (2017).
47. Li, L. et al. High-performance solid-state supercapacitors and micro-supercapacitors derived from printable graphene inks. *Adv. Energy Mater.* **6**, 1600909 (2016).
48. Liu, Y. et al. Development of graphene oxide/polyaniline inks for high performance flexible microsupercapacitors via extrusion printing. *Adv. Funct. Mater.* **28**, 1706592 (2018).
49. Zhang, C. J. et al. Additive-free MXene inks and direct printing of micro-supercapacitors. *Nat. Commun.* **10**, 1795 (2019).
50. Wang, Y., Zhang, Y.-Z., Gao, Y.-Q., Sheng, G. & ten Elshof, J. E. Defect engineering of MnO_2 nanosheets by substitutional doping for printable solid-state micro-supercapacitors. *Nano Energy* **68**, 104306 (2020).

51. Pang, H., Zhang, Y., Lai, W.-Y., Hu, Z. & Huang, W. Lamellar $K_2Co_3(P_2O_7)_2{\cdot}2H_2O$ nanocrystal whiskers: high-performance flexible all-solid-state asymmetric micro-supercapacitors via inkjet printing. *Nano Energy* **15**, 303–312 (2015).
52. Cheng, T. et al. Inkjet-printed high-performance flexible micro-supercapacitors with porous nanofiber-like electrode structures. *Small* **15**, 1901830 (2019).
53. Niu, Z. et al. All-solid-state flexible ultrathin micro-supercapacitors based on graphene. *Adv. Mater.* **25**, 4035–4042 (2013).
54. Kurra, N., Hota, M. K. & Alshareef, H. N. Conducting polymer micro-supercapacitors for flexible energy storage and Ac line-filtering. *Nano Energy* **13**, 500–508 (2015).
55. Hong, S. Y. et al. High-density, stretchable, all-solid-state microsupercapacitor arrays. *ACS Nano* **8**, 8844–8855 (2014).
56. Wu, Z.-K. et al. Flexible micro-supercapacitor based on in-situ assembled graphene on metal template at room temperature. *Nano Energy* **10**, 222–228 (2014).
57. Sun, L., Wang, X., Zhang, K., Zou, J. & Zhang, Q. Metal-free SWNT/carbon/MnO_2 hybrid electrode for high performance coplanar micro-supercapacitors. *Nano Energy* **22**, 11–18 (2016).
58. Hong, X. et al. Microstructuring of carbon/tin quantum dots via a novel photolithography and pyrolysis-reduction process. *Nano Res.* **10**, 3743–3753 (2017).
59. Tian, X. et al. Vertically stacked holey graphene/polyaniline heterostructures with enhanced energy storage for on-chip micro-supercapacitors. *Nano Res.* **9**, 1012–1021 (2016).
60. Cao, L. et al. Direct laser-patterned micro-supercapacitors from paintable MoS_2 films. *Small* **9**, 2905–2910 (2013).
61. Gao, J. et al. Laser-assisted large-scale fabrication of all-solid-state asymmetrical micro-supercapacitor array. *Small* **14**, 1801809 (2018).
62. Zhang, L. et al. Flexible micro-supercapacitor based on graphene with 3D structure. *Small* **13**, 1603114 (2017).
63. Wang, N. et al. Laser-cutting fabrication of MXene-based flexible micro-supercapacitors with high areal capacitance. *ChemNanoMat* **5**, 658–665 (2019).
64. Ye, J. et al. Direct laser writing of graphene made from chemical vapor deposition for flexible, integratable micro-supercapacitors with ultrahigh power output. *Adv. Mater.* **30**, 1801384 (2018).
65. Peng, Z. et al. Flexible boron-doped laser-induced graphene micro-supercapacitors. *ACS Nano* **9**, 5868–5875 (2015).
66. Shi, X. et al. One-step scalable fabrication of graphene-integrated micro-supercapacitors with remarkable flexibility and exceptional performance uniformity. *Adv. Funct. Mater.* **29**, 1902860 (2019).
67. Li, L. et al. High-performance pseudocapacitive microsupercapacitors from laser-induced graphene. *Adv. Mater.* **28**, 838–845 (2016).
68. Brousse, K. et al. Facile and scalable preparation of ruthenium oxide-based flexible micro-supercapacitors. *Adv. Energy Mater.* **10**, 1903136 (2019).
69. Jiang, K. et al. Interfacial approach toward benzene-bridged polypyrrole film–based micro-supercapacitors with ultrahigh volumetric power density. *Adv. Funct. Mater.* **30**, 1908243 (2019).
70. Xiao, H. et al. One-step device fabrication of phosphorene and graphene interdigital micro-supercapacitors with high energy density. *ACS Nano* **11**, 7284–7292 (2017).
71. Zheng, S. et al. All-solid-state planar integrated lithium ion micro-batteries with extraordinary flexibility and high-temperature performance. *Nano Energy* **51**, 613–620 (2018).
72. Huang, X. & Wu, P. A facile, high-yield, and freeze-and-thaw-assisted approach to fabricate MXene with plentiful wrinkles and its application in on-chip micro-supercapacitors. *Adv. Funct. Mater.* **30**, 1910048 (2020).
73. Qin, J. et al. 2D mesoporous MnO_2 nanosheets for high-energy asymmetric micro-supercapacitors in water-in-salt gel electrolyte. *Energy Storage Mater.* **18**, 397–404 (2019).
74. Zheng, S. et al. All-solid-state planar sodium-ion microcapacitors with multi-directional fast ion diffusion pathways. *Adv. Sci.* **6**, 1902147 (2019).
75. Zhang, C. J. et al. Stamping of flexible, coplanar micro-supercapacitors using MXene inks. *Adv. Funct. Mater.* **28**, 1705506 (2018).
76. Zhu, S., Li, Y., Zhu, H., Ni, J. & Li, Y. Pencil-drawing skin-mountable micro-supercapacitors. *Small* **15**, 1804037 (2019).
77. Salles, P., Quain, E., Kurra, N., Sarycheva, A. & Gogotsi, Y. Automated scalpel patterning of solution processed thin films for fabrication of transparent MXene microsupercapacitors. *Small* **14**, 1802864 (2018).
78. Li, J. et al. MXene-conducting polymer electrochromic microsupercapacitors. *Energy Storage Mater.* **20**, 455–461 (2019).
79. Xiong, G., Meng, C., Reifenberger, R. G., Irazoqui, P. P. & Fisher, T. S. A review of graphene-based electrochemical microsupercapacitors. *Electroanalysis* **26**, 30–51 (2014).
80. Xu, Q., Pang, H., Xue, H., Li, Q. & Zheng, S. A highly alkaline-stable metal oxide@metal–organic framework composite for high-performance electrochemical energy storage. *Natl Sci. Rev.* **7**, 305–314 (2020).
81. Li, Y., Xu, Y., Liu, Y. & Pang, H. Exposing {001} crystal plane on hexagonal Ni-MOF with surface-grown cross-linked mesh-structures for electrochemical energy storage. *Small* **15**, 1902463 (2019).
82. Najib, S. & Erdem, E. Current progress achieved in novel materials for supercapacitor electrodes: mini review. *Nanoscale Adv.* **1**, 2817–2827 (2019).
83. Beidaghi, M. & Wang, C. Micro-supercapacitors based on interdigital electrodes of reduced graphene oxide and carbon nanotube composites with ultrahigh power handling performance. *Adv. Funct. Mater.* **22**, 4501–4510 (2012).
84. Meng, Q. et al. High-performance all-carbon yarn micro-supercapacitor for an integrated energy system. *Adv. Mater.* **26**, 4100–4106 (2014).
85. In, J. B. et al. Facile fabrication of flexible all solid-state micro-supercapacitor by direct laser writing of porous carbon in polyimide. *Carbon* **83**, 144–151 (2015).
86. Liu, W.-W., Feng, Y.-Q., Yan, X.-B., Chen, J.-T. & Xue, Q.-J. Superior micro-supercapacitors based on graphene quantum dots. *Adv. Funct. Mater.* **23**, 4111–4122 (2013).
87. Hsia, B. et al. Highly flexible, all solid-state micro-supercapacitors from vertically aligned carbon nanotubes. *Nanotechnology* **25**, 055401 (2014).
88. Lu, A.-K., Li, H.-Y. & Yu, Y. Holey graphene synthesized by electrochemical exfoliation for high-performance flexible microsupercapacitors. *J. Mater. Chem. A* **7**, 7852–7858 (2019).
89. Liu, Z. et al. Ultraflexible in-plane micro-supercapacitors by direct printing of solution-processable electrochemically exfoliated graphene. *Adv. Mater.* **28**, 2217–2222 (2016).
90. Bellani, S. et al. Scalable production of graphene inks via wet-jet milling exfoliation for screen-printed micro-supercapacitors. *Adv. Funct. Mater.* **29**, 1807659 (2019).
91. Ma, R., Gordon, D., Yushin, G. & Tsukruk, V. V. Robust and flexible micropatterned electrodes and micro-supercapacitors in graphene-silk biopapers. *Adv. Mater. Interfaces* **5**, 1801203 (2018).
92. Li, Y. et al. High performance nanoporous carbon microsupercapacitors generated by a solvent-free MOF-CVD method. *Carbon* **152**, 688–696 (2019).
93. Wang, Y. et al. Direct graphene-carbon nanotube composite ink writing all-solid-state flexible microsupercapacitors with high areal energy density. *Adv. Funct. Mater.* **30**, 1907284 (2020).
94. Wu, Z.-S. et al. Layer-by-layer assembled heteroatom-doped graphene films with ultrahigh volumetric capacitance and rate capability for micro-supercapacitors. *Adv. Mater.* **26**, 4552–4558 (2014).
95. Liu, Z. et al. High power in-plane micro-supercapacitors based on mesoporous polyaniline patterned graphene. *Small* **13**, 1603388 (2017).
96. Park, H. et al. Microporous polypyrrole-coated graphene foam for high-performance multifunctional sensors and flexible supercapacitors. *Adv. Funct. Mater.* **28**, 1707013 (2018).
97. Zhu, M. et al. A highly durable, transferable, and substrate-versatile high-performance all-polymer micro-supercapacitor with plug-and-play function. *Adv. Mater.* **29**, 1605137 (2017).
98. Hu, H., Zhang, K., Li, S., Ji, S. & Ye, C. Flexible, in-plane, and all-solid-state micro-supercapacitors based on printed interdigital Au/polyaniline network hybrid electrodes on a chip. *J. Mater. Chem. A* **2**, 20916–20922 (2014).
99. Wang, K. et al. An all-solid-state flexible micro-supercapacitor on a chip. *Adv. Energy Mater.* **1**, 1068–1072 (2011).
100. Say, M. G. et al. Spray-coated paper supercapacitors. *npj Flex. Electron.* **4**, 14 (2020).
101. Wang, X., Yin, Y., Li, X. & You, Z. Fabrication of a symmetric micro supercapacitor based on tubular ruthenium oxide on silicon 3D microstructures. *J. Power Sources* **252**, 64–72 (2014).
102. Xue, M. et al. Microfluidic etching for fabrication of flexible and all-solid-state micro supercapacitor based on MnO_2 nanoparticles. *Nanoscale* **3**, 2703–2708 (2011).
103. Xu, H. et al. Flexible asymmetric micro-supercapacitors based on Bi_2O_3 and MnO_2 nanoflowers: larger areal mass promises higher energy density. *Adv. Energy Mater.* **5**, 1401882 (2015).
104. Eustache, E. et al. High areal energy 3D-interdigitated micro-supercapacitors in aqueous and ionic liquid electrolytes. *Adv. Mater. Technol.* **2**, 1700126 (2017).
105. Xu, J. et al. Ultrathin Cu-MOF@δ-MnO_2 nanosheets for aqueous electrolyte-based high-voltage electrochemical capacitors. *J. Mater. Chem. A* **6**, 17329–17336 (2018).
106. Lei, Z. et al. Nanoelectrode design from microminiaturized honeycomb monolith with ultrathin and stiff nanoscaffold for high-energy micro-supercapacitors. *Nat. Commun.* **11**, 299 (2020).
107. Pang, J. et al. Applications of 2D MXenes in energy conversion and storage systems. *Chem. Soc. Rev.* **48**, 72–133 (2019).
108. Anasori, B., Lukatskaya, M. R. & Gogotsi, Y. 2D metal carbides and nitrides (MXenes) for energy storage. *Nat. Rev. Mater.* **2**, 16098 (2017).
109. Nan, J. et al. Nanoengineering of 2D MXene-based materials for energy storage applications. *Small* **10**, 1902085 (2019).
110. VahidMohammadi, A., Mojtabavi, M., Caffrey, N. M., Wanunu, M. & Beidaghi, M. Assembling 2D MXenes into highly stable pseudocapacitive electrodes with high power and energy densities. *Adv. Mater.* **31**, 1806931 (2019).

111. Kurra, N., Ahmed, B., Gogotsi, Y. & Alshareef, H. N. MXene-on-paper coplanar microsupercapacitors. *Adv. Energy Mater.* **6**, 1601372 (2016).
112. Huang, H. et al. Extraordinary areal and volumetric performance of flexible solid-state micro-supercapacitors based on highly conductive freestanding $Ti_3C_2T_X$ films. *Adv. Electron. Mater.* **4**, 1800179 (2018).
113. Li, H., Li, X., Liang, J. & Chen, Y. Hydrous RuO_2-decorated MXene coordinating with silver nanowire inks enabling fully printed micro-supercapacitors with extraordinary volumetric performance. *Adv. Energy Mater.* **9**, 1803987 (2019).
114. Chen, X. et al. Direct laser etching free-standing MXene-MoS_2 film for highly flexible micro-supercapacitor. *Adv. Mater. Interfaces* **6**, 1901160 (2019).
115. Zhu, Y. et al. Modifications of MXene layers for supercapacitors. *Nano Energy* **73**, 104734 (2020).
116. Shao, Y. et al. Design and mechanisms of asymmetric supercapacitors. *Chem. Rev.* **118**, 9233–9280 (2018).
117. Zhu, Q. et al. A new view of supercapacitors: integrated supercapacitors. *Adv. Energy Mater.* **9**, 1901081 (2019).
118. Liu, W. et al. Advanced electrode materials comprising of structure-engineered quantum dots for high-performance asymmetric micro-supercapacitors. *Adv. Energy Mater.* **10**, 1903724 (2020).
119. Couly, C. et al. Asymmetric flexible MXene-reduced graphene oxide micro-supercapacitor. *Adv. Electron. Mater.* **4**, 1700339 (2018).
120. Zuo, W. et al. Battery-supercapacitor hybrid devices: recent progress and future prospects. *Adv. Sci.* **4**, 1600539 (2017).
121. Zhang, P. et al. Zn-ion hybrid micro-supercapacitors with ultrahigh areal energy density and long-term durability. *Adv. Mater.* **31**, 1806005 (2018).
122. Li, W., Meredov, A. & Shamim, A. Coat-and-print patterning of silver nanowires for flexible and transparent electronics. *npj Flex. Electron.* **3**, 19 (2019).
123. Zhao, C., Liu, Y., Beirne, S., Razal, J. & Chen, J. Recent development of fabricating flexible micro-supercapacitors for wearable devices. *Adv. Mater. Technol.* **3**, 1800028 (2018).
124. Pu, X., Hu, W. & Wang, Z. L. Toward wearable self-charging power systems: the integration of energy-harvesting and storage devices. *Small* **14**, 1702817 (2018).
125. Luo, J. et al. Integration of micro-supercapacitors with triboelectric nanogenerators for a flexible self-charging power unit. *Nano Res.* **8**, 3934–3943 (2015).
126. Zhang, S. L. et al. Energy harvesting-storage bracelet incorporating electrochemical microsupercapacitors self-charged from a single hand gesture. *Adv. Energy Mater.* **9**, 1900152 (2019).
127. Jiang, Q. et al. MXene electrochemical microsupercapacitor integrated with triboelectric nanogenerator as a wearable self-charging power unit. *Nano Energy* **45**, 266–272 (2018).
128. Yun, J. et al. A patterned graphene/ZnO UV sensor driven by integrated asymmetric micro-supercapacitors on a liquid metal patterned foldable paper. *Adv. Funct. Mater.* **27**, 1700135 (2017).
129. Kaidarova, A. et al. Wearable multifunctional printed graphene sensors. *npj Flex. Electron.* **3**, 15 (2019).
130. Yun, J. et al. Stretchable patterned graphene gas sensor driven by integrated micro-supercapacitor array. *Nano Energy* **19**, 401–414 (2016).
131. Qin, J. et al. Hierarchical ordered dual-mesoporous polypyrrole/graphene nanosheets as bi-functional active materials for high-performance planar integrated system of micro-supercapacitor and gas sensor. *Adv. Funct. Mater.* **30**, 1909756 (2020).
132. Song, Y. et al. All-in-one piezoresistive-sensing patch integrated with micro-supercapacitor. *Nano Energy* **53**, 189–197 (2018).
133. Yun, J. et al. Stretchable array of high-performance micro-supercapacitors charged with solar cells for wireless powering of an integrated strain sensor. *Nano Energy* **49**, 644–654 (2018).
134. Moon, Y. S. et al. Fabrication of flexible micro-supercapacitor array with patterned graphene foam/MWNT-COOH/MnO_X electrodes and its application. *Carbon* **81**, 29–37 (2015).
135. Guo, R. et al. In-plane micro-supercapacitors for an integrated device on one piece of paper. *Adv. Funct. Mater.* **27**, 1702394 (2017).
136. Cai, J., Lv, C. & Watanabe, A. Laser direct writing of high-performance flexible all-solid-state carbon micro-supercapacitors for an on-chip self-powered photodetection system. *Nano Energy* **30**, 790–800 (2016).
137. Gao, C. et al. A directly swallowable and ingestible micro-supercapacitor. *J. Mater. Chem. A* **8**, 4055–4061 (2020).
138. Lu, Y., Jiang, K., Chen, D. & Shen, G. Wearable sweat monitoring system with integrated micro-supercapacitors. *Nano Energy* **58**, 624–632 (2019).
139. Zhao, D. et al. Charge transfer salt and graphene heterostructure-based micro-supercapacitors with alternating current line-filtering performance. *Small* **15**, 1901494 (2019).
140. Yang, C. et al. Coordination polymer framework based on-chip micro-supercapacitors with AC line-filtering performance. *Angew. Chem. Int. Ed. Engl.* **56**, 3920–3924 (2017).
141. Xu, S., Liu, W., Hu, B. & Wang, X. Circuit-integratable high-frequency micro supercapacitors with filter/oscillator demonstrations. *Nano Energy* **58**, 803–810 (2019).
142. Jiang, Q. et al. On-chip MXene microsupercapacitors for AC-line filtering applications. *Adv. Energy Mater.* **9**, 1901061 (2019).
143. Wu, Y., Hu, H., Yuan, C., Song, J. & Wu, M. Electrons/ions dual transport channels design: concurrently tuning interlayer conductivity and space within re-stacked few-layered MXenes film electrodes for high-areal-capacitance stretchable micro-supercapacitor-arrays. *Nano Energy* **74**, 104812 (2020).

ACKNOWLEDGEMENTS

The authors acknowledge the financial supports by National Natural Science Foundation of China (Grant No. 51902265), Fundamental Research Funds for the Central Universities, Key Research and Development Program of Shaanxi (Program No.2020KWZ-001), and Project for graduate Innovation team of Northwestern Polytechnical University.

AUTHOR CONTRIBUTIONS

F.B., W.W.Z., and C.G. conceptualized the work. F.B., W.W.Z., Y.H.X., Y.D., C.G., and W.H. collected the data and contributed to paper writing. All the authors participated in the scientific discussion. F.B. and W.W.Z. are co-first authors.

COMPETING INTERESTS

The authors declare no competing interests.

ADDITIONAL INFORMATION

Correspondence and requests for materials should be addressed to C.G. or W.H.

Reprints and permission information is available at http://www.nature.com/reprints

Publisher's note Springer Nature remains neutral with regard to jurisdictional claims in published maps and institutional affiliations.